Arctic mutant amyloid β protein interferes the functions of CHRNA7 through specific binding

Arctic 変異型アミロイドβ蛋白による CHRNA7 機能の抑制とその分子メカニズムの解析

February 2017

Ye JU

琚 曄

Arctic mutant amyloid β protein interferes the functions of CHRNA7 through specific binding

Arctic 変異型アミロイドβ蛋白による CHRNA7 機能の抑制とその分子メカニズムの解析

February 2017

Waseda University
Graduate School of Advanced Science and Engineering
Department of Life science and Medical Bioscience,
Research on Bio-Solid State Science

Ye JU

琚 曄

Contents

Chapter 1 Introduction

Alzheimer's disease (AD), with -26,000,000 patients worldwide, constitutes the most common neurodegenerative disorder. The number of people who suffer from AD is expected to reach -106,000,000 by 2050 if no preventive treatments become available (Brookmeyer et al. 2007; Dziewczapolski et al. 2009). AD describes a set of symptoms, which includes the loss of memory, mood changes, problems with communication and reasoning. AD, which first described by the German neurologist Alois Alzheimer, is a physical disease affecting the brains. The neuropathological and neurochemical hallmarks of AD include: synaptic loss and selective neuronal cell-death; decrease of the markers for certain neurotransmitters; and abnormalities in neurons and their processes as well as in the extracellular space (Haass & Selkoe 2007; Roberson & Mucke 2006). Among the course of the disease, 'senile plaques' and 'neurofibrillary tangles' are developed within the structure of the brains, leading to the death of brain cells.

There are several hypotheses about AD pathology causes, among which the 'amyloid hypothesis' is the main basic hypothesis for most of the researches. The traditional formulation of amyloid hypothesis suggests that the cytotoxicity of mature aggregated amyloid fibrils are believed to be the toxic form of the protein, responsible for disrupting the cellular calcium ion

homeostasis and thereby inducing apoptosis (Yankner et al. 1990). That means, the accumulation of amyloid beta protein (Aβ) fragments in the brain trigger the disruption and destruction of nerve cells that cause AD. This hypothesis is supported by the observation that a variant of Aβ known to form senile plaque (Glenner & Wong 1984). Aβ peptides are thus considered to play a significant role in the pathogenesis of AD because of their ability to aggregate into β-sheets, which constitute the amyloid plaques in AD brains (Burdick et al. 1992). (Figure 1-1) Aβ assemblies can be mainly divided into 2 big groups: insoluble fibrillary structure, which are mainly found in senile plaque, and soluble non-fibrillar structures with a wide molecular weight range (from <10kDa to >100kDa) (Sakono & Zako 2010). Soluble non-fibrillar structures include several different types of oligomers such as very short oligomers ranging from dimer to hexamer size and Aβ-derived diffusible ligands (ADDLs) ranging from 17 to 42 kDa (Kirkitadze & Kowalska 2005), and larger nonfibrillar aggregates known as protofibrils (Sandberg et al. 2010). Among those, soluble non-fibrillar structures have been reported to be highly toxic in neurons with increased neuronal death (Dahlgren et al. 2002; Sakono & Zako 2010), and causing synaptic dysfunction through calcium impairment, long term potentiation (LTP) blockage and synapse loss (Shankar & Walsh 2009; Tu et al. 2014; Palop & Mucke 2010).

Aβ is formed after sequential cleavage of the amyloid precursor protein (APP) by β- and γ- secretase. The γ-secretase, which produces the C-terminal end of the Aβ peptide, cleaves within the transmembrane region of APP and generates a number of isoforms of 36-43 amino acid residues in length. The most common isoforms are Aβ40 and Aβ42 (Haass 2004; Figure 1-2A). Even though Aβ42 has been reported to be the more neurotoxic (Jarrett et al. 1993) and more hydrophobic isoform, which prone to form aggregates more easily, Aβ40 is the predominant one and the main compose of senile plaque (Hsiao et al. 1996; Selkoe 1998).

Several autosomal dominant mutations causing early-onset familial AD (FAD) have been identified in the APP gene, suggesting that this protein affects either the metabolism of Aβ or its properties of aggregation (Selkoe 1999; Ronnback et al. 2012). Those mutations cause a rapidly and progressive and severe form of the disease (Bertram & Tanzi 2004; Whalen et al. 2005). Clinical features of FAD are indistinguishable from those of sporadic cases; however, disease onset occurs at a much younger age (Kamino et al. 1992). Point mutations in the Aβ sequence associated with FAD are clustered around the central hydrophobic core of Aβ (Figure 1-2B). The ‘Dutch’ mutation in the Aβ sequence, Aβ[E22Q] gives rise to a highly distinct phenotype of severe amyloid angiopathy, leading to recurrent cerebral hemorrhage (Van Broeckhoven et al. 1990). The ‘Iowa’ mutation,

Aβ[D23N], is associated with severe amyloid angiopathy as well (Grabowski et al. 2001). The Aβ[E22G] mutation, found to cause AD in Swedish families, was first reported in 2001 by Nilsberth et al., is named the Arctic mutation (Nilsberth et al. 2001). This mutation has a purely cognitive phenotype, typical of AD, without showing the presence of marked amyloid angiopathy (Basun et al. 2008). Carriers of the Arctic mutation have decreased amounts of plasma Aβ(1-42) and Aβ(1-40), and demonstrated that Aβ(1-40)E22G forms protofibrils much faster and more abundantly than the wild-type Aβ, whereas the rate of fibrillization remains the same (Nilsberth et al. 2001; Itkin et al. 2011). There were other aspects of aggregation patterns of Arctic Aβ being studied as well. Oligomerization pattern of Arctic mutation was reported different from wild type Aβ with a tendency to form larger oligomers (Gessel et al. 2012). Fibril structures were also observed and studied previously (Norlin et al. 2012). Therefore, special aggregation pattern of Arctic Aβ has been suggested to be a primary result of 'Arctic' mutation.

The nicotinic acetylcholine receptors, key players in neuronal communication, convert neurotransmitter binding into membrane electrical depolarization. One of the receptors, alpha-7 nicotinic acetylcholine receptor, is composed of homologous subunits known as neuronal acetylcholine receptor subunit alpha-7 (CHRNA7). This receptor is mainly located in the brain where activation yields pre- and postsynaptic excitation,

mainly by increased Ca^{2+} permeability (Bertrand et al. 1993; Figure 1-3). CHRNA7 regulates numerous Ca^{2+}-dependent events in the nervous system (Liu et al. 2001; Séguéla et al. 1993), and its activation can mediate long-term potentiation (LTP) at glutamatergic synapses (Mansvelder & McGehee 2000). CHRNA7 has been reported to show the neuroprotective function by its activation, both *in vitro* (Qi et al. 2007; Martin et al. 2004) and *in vivo* (Di Cesare Mannelli et al. 2014; Liu et al. 2012) as well.

Previous studies have found that Aβ42 binds to CHRNA7 with high affinity (H. Wang et al. 2000; H.-Y. Wang et al. 2000). Furthermore, the decline of senile plaques has been detected in Aβ-over-expressed transgene mice by blocking of CHRNA7 (Dziewczapolski et al. 2009). Moreover, Aβ has been found to interact with CHRNA7 resulting in impaired receptor functions (Pettit et al. 2001; Liu et al. 2001). Meanwhile, Aβ has been reported to enhance its aggregation in the lipid raft with CHRNA7 exiting in it (Ehehalt et al. 2003; Brusés et al. 2001). Combine together, these results have led to the hypothesis that the CHRNA7 subunit plays a role in AD.

Because the molecular mechanism of Arctic mutation-mediated FAD remains unknown, Arctic Aβ and CHRNA7 were investigated (Ju et al. 2014). *In vitro* binding assay was performed to search the direct interaction between CHRNA7 and Arctic Aβ, Thioflavin T (ThT) assay and transmission

electron microscopy to test the aggregation ability of Arctic Aβ with or without the addition of CHRNA7, and measured Ca^{2+} response to nicotine induction and its downstream signal ERK1/2 activation to analyze whether the function of CHRNA7 was influenced by Arctic Aβ (Ju et al. 2014). Furthermore, whether Arctic Aβ could affect the neuroprotective effect of CHRNA7 was searched by using MTS assay and fluorescence microscopy. Human neuroblastoma (SH-SY5Y) cells were used.

Several different signaling cascades are reported to be participating in cell survival within nicotine anti-apoptotic action, including the extracellular signal-regulated kinase/mitogen-activated protein kinase (ERK1/2) pathway (Ren et al. 2005; Toborek et al. 2007), the JNK pathway (Huang et al. 2012), as well as v-akt murin thymoma viral oncogene homolog (AKT) pathway (Kihara et al. 2001; Buckinham et al. 2009). The activation of those signaling proteins was investigated to assist the further understanding of molecular mechanism of Arctic-mediated FAD through CHRNA7 by biochemical assay.

This study indicated the novel understanding of the molecular mechanism of Arctic mutation-mediated FAD.

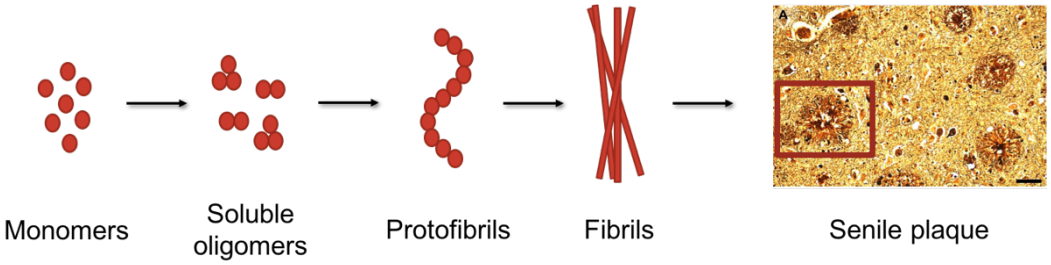

Figure 1-1 Amyloid β proteins accumulate to form senile plaque

Senile plaques are found in Alzheimer's disease patients' brains (Image from Miller & Boeve 2009). Senile plaques are mainly composed of Amyloid β. This Aβ proteins aggregate, from monomers, throughout oligomers, protofribrils and fibrils structures, eventually to form plaques.

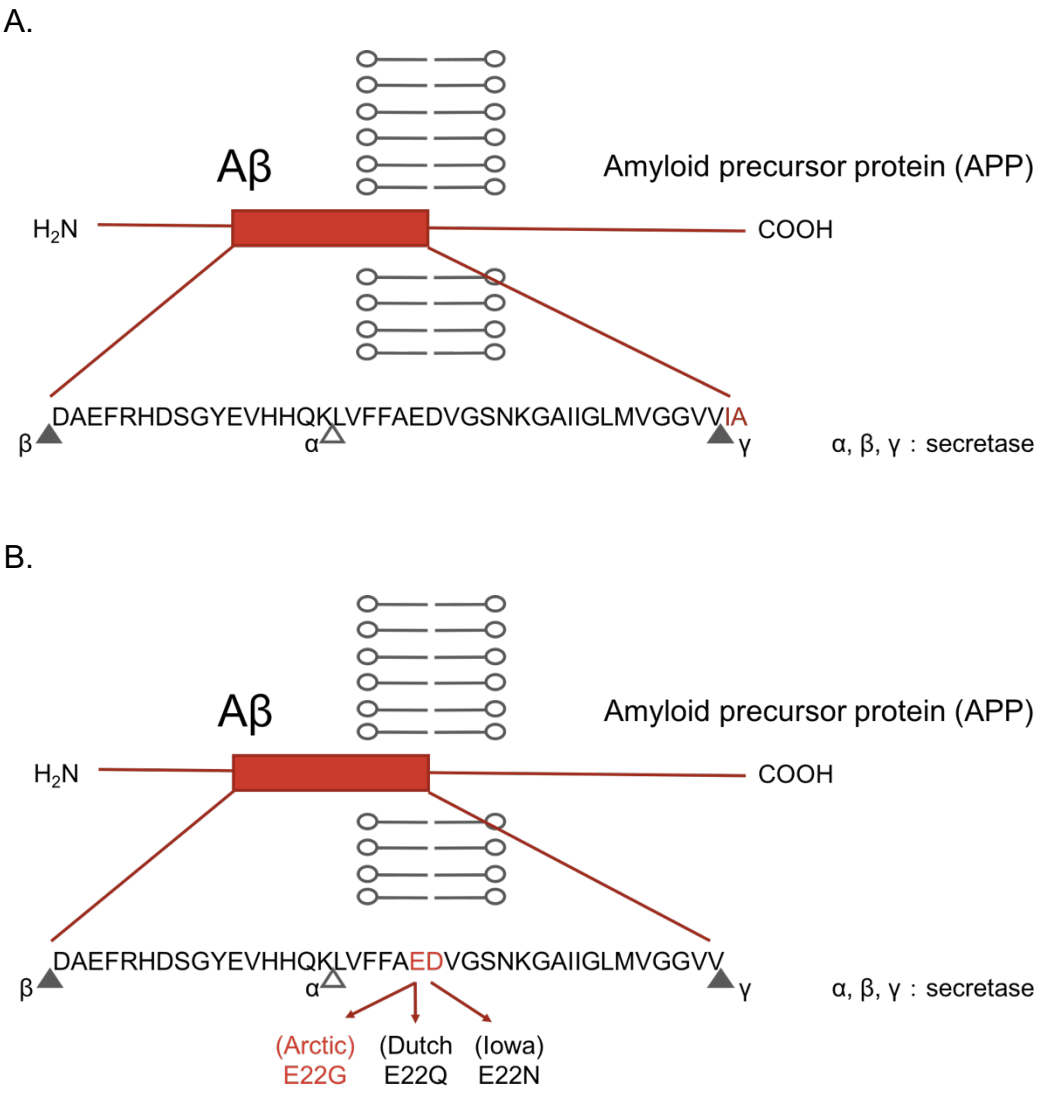

Figure 1-2 Different isoforms of Amyloid β protein

Amyloid β has different isoforms. (A) Different isoforms of Amyloid β protein are named based on different amino acid residues in length, generated by sequential cleavage difference by γ-secretase from Amyloid precursor protein (APP). Even though Aβ42 has been reported to be the more neurotoxic (Jarrett et al. 1993) and more hydrophobic isoform, which prone to form aggregates more easily, Aβ40 is the predominant one and the main

compose of senile plaque (Hsiao et al. 1996; Selkoe 1998). (B) Mutant forms of Aβ40 are generated by single amino acid mutation in Aβ40 sequence, causing different types of familial Alzheimer's disease (FAD). (E22Q: Dutch mutation; D23N: Iowa mutation; E22G; Arctic mutation)

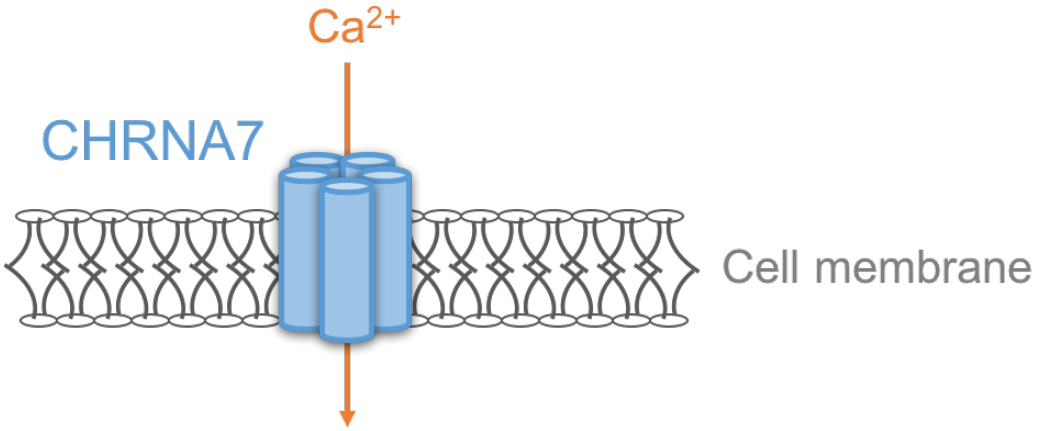

Figure 1-3 CHRNA7 regulates Ca^{2+} permeability

CHRNA7 is mainly located in the brain where activation yields pre- and postsynaptic excitation, mainly by increased Ca^{2+} permeability (Bertrand et al. 1993). CHRNA7 regulates numerous Ca^{2+}-dependent events in the nervous system (Liu et al. 2001; Séguéla et al. 1993), and its activation can mediate long-term potentiation (LTP) at glutamatergic synapses (Mansvelder & McGehee 2000).

Chapter 2 Methods and Materials

2-1 Cell culture

Chinese hamster ovary (CHO-K1) cell lines and SH-SY5Y human neuroblastoma cell lines were used in this research. Cell culture media was D-MEM (low Glucose) (Dulbecco's Modified Eagle's Medium, Wako, Osaka, Japan) containing FBS (Fetal bovine serum, 10%) (Thermo Fisher Scientific, San Jose, CA, USA) and Penicillin-Streptomycin Solution (1%).

2-2 Antibodies

The following antibodies were used as primary antibodies: anti-CHRNA7 polyclonal antibody (Santa Cruz Biotechnology, Dallas, TX, USA); anti-Glutathione S-transferase monoclonal antibody (Wako); Aβ monoclonal antibody 6E10 (Covance, Berkeley, CA, USA); p44/42 MAPK (ERK1/2) Rabbit monoclonal antibody (Cell Signaling Technology, Beverly, MA, USA); Phospho-p44/42 MAPK (ERK1/2) (Thr202/Tyr204) Rabbit monoclonal antibody (Cell Signaling Technology); anti-HA-tag polyclonal antibody (Medical & Biological laboratories, Nagoya, Japan); Phospho-SAPK/JNK (Thr 183/Tyr 185) antibody (Cell Signaling Technology); SAPK/JNK antibody (Cell Signaling Technology); Akt (pan) (C67E7) Rabbit monoclonal antibody (Cell Signaling Technology); Phospho-Akt (Ser473)

Rabbit monoclonal antibody (Cell Signaling Technology); anti-β actin monoclonal antibody (Wako).

The following antibodies were used as secondary antibodies: ZyMax^{TM} Rabbit anti-Goat IgG (H+L) HRP Conjugate (Invitrogen, Carlsbad, CA USA); ECL^{TM} Anti-mouse IgG, Horseradish Peroxidase linked whole antibody (GE Healthcare UK Limited, Buckinghamshire, UK); ECL^{TM} Anti-Rabbit IgG, Horseradish Peroxidase linked whole antibody (GE Healthcare UK Limited).

2-3 Preparation of Aβ

The synthesized wild-type Aβ proteins (Human 1-40, Human 1-42) and the mutant Aβ proteins (Arctic[E22G], Dutch[E22Q], and Iowa [D23N]) were used for the *in vitro* binding assay, and were purchased from Anaspec (Fremont, CA, USA). Arctic Aβ40 used in Thioflavin T assay, Ca^{2+} flux measurement and biochemical assay was purchased from Bachem (Torrance, CA, USA), which used in MTS cell proliferation assay and fluorescence microscopy was purchased from Anaspec. All amyloid peptides were dissolved in 0.1% ammonia to 1mM, then diluted to 100μM in phosphate-buffered saline (PBS).

2-4 Transfection

PEI-MAX (Polysciences Inc., Warrington, PA USA) was utilized for gene transfection into the cells. Serum-free medium was mixed by vortex after the introduction of plasmid vectors. With the incubation in room temperature for 10 minutes, the transfection solutions were added into cell culture media. The further experiments were performed after 24h to 48h with the maximum expression level.

2-5 Construction of plasmid vectors

2-5-1 Construction of CHRNA7 expression vector for protein preparation

Mammalian Gene Collection Human CHRNA7 sequence-verified cDNA was purchased from Open Biosystems (Huntsville, AL, USA). CHRNA7 cDNAs were amplified from this cDNA, and SalI/NotI fragments containing CHRNA7 were isolated and ligated into the mammalian expression vector, pGEX-4T-3 GST, digested with the same endonucleases. The resulting recombinant plasmid, GST-CHRNA7 was cultured and induced by isopropyl-ß-D- thiogalactoside (IPTG) (1mM) (Wako, Osaka, Japan) for protein expression. For purification, GST-CHRNA7 protein was collected and bound to Glutathion-Sepharose 4B (Wako), then eluted by elution buffer (100mM Tris-HCl pH8.7, 20mM Glutathion).

2-5-2 Construction of CHRNA7 expression vectors for transfection

Mammalian Gene Collection Human CHRNA7 sequence-verified cDNA was purchased from Open Biosystems (Huntsville, AL, USA). CHRNA7 cDNAs were amplified from this cDNA, and SalI/NotI fragments containing CHRNA7 were isolated and ligated into the mammalian expression vector, pRK5-HA, digested with the same endonucleases. The resulting recombinant plasmid, pRK5-HA-CHRNA7 was used for further studies. The entire nucleotide sequence was confirmed by DNA sequencing.

2-5-3 Construction of RNAi vectors for transfection

A vector system for small hairpin RNAs (shRNAs) was used to suppress endogenous CHRNA7 protein expression (pSilencer Vectors, Life Technologies). I generated shRNA plasmids using the following sequences: shRNA1 duplex contained 5'-CGUGGCCAAUGACUCGCAAtt-3' as the sense and 5'-UUGCGAGUCAUUGGCCACGgg-3' as the anti-sense sequence; shRNA2 duplex contained 5'-CCAACAUUUGGCUGCAAAUtt-3' as the sense and 5'-AUUUGCAGCCAAAUGUUGGtg-3' as the anti-sense sequence. Scramble shRNA that does not target any endogenous transcript was employed to control for non-specific effects.

2-6 *In vitro* binding assay

GST-CHRNA7 was co-incubated with synthetic Aβ at 4°C for 2 h in 1 mL of binding buffer. For immunoprecipitation, anti-CHRNA7 antibodies were coupled to protein G Mag Sepharose beads (5 μL) (GE Healthcare, Waukesha, WI, USA) via a 1h incubation at 4°C. The samples were incubated with magnetic beads for 1h at 4°C, washed three times with PBS, eluted with sample buffer solution (Wako), and quantified via western blotting.

2-7 Western blotting

A standard protocol (Sawamura et al. 2001; Sawamura et al. 2005) was used but with minor modifications. Proteins were separated using SuperSep gels (Wako) and transferred to polyvinylidene difluoride membranes (Millipore, Billerica, MA, USA). Nonspecific binding was then blocked with 5% skim milk (Wako) containing 0.1% Tween 20 (Bio-Rad Laboratories, Hercules, CA, USA) in PBS. Membranes were then incubated with primary antibodies overnight at 4°C. For the detection of both monoclonal and polyclonal antibodies, appropriate peroxidase-conjugated secondary antibodies were used in conjunction with Novex ECL (Life Technologies). Images were recorded with the LAS-3000 imager (Fujifilm, Tokyo, Japan), and ImageJ (NIH) was used as an automatic image analysis software.

2-8 Thioflavin T (ThT) Assay

The degree of Aβ aggregation was determined using the fluorescent dye, ThT (LeVine 1993). Thioflavin T (ThT), one of the benzathiole dye, is described as a potent fluorescent marker of amyloid in histology (Figure 2-1;Biancalana & Koide 2010). ThT selectively localizes to amyloid deposits, thereupon exhibiting a dramatic increase in fluorescent brightness. Upon binding of fibrils, ThT displays a dramatic shift of the excitation maximum (from 385 nm to 450 nm) and the emission maximum (from 445 nm to 482 nm) and that ThT fluorescence originates only from the dye bound to amyloid fibrils (LeVine 1993; Biancalana & Koide 2010). The incubated sample (10 μL) was taken every 3 h, treated with 100 μM ThT, and adjusted to 50 mM with glycine NaOH buffer (pH 8.5). Absorbance was measured at an excitation and emission wavelength of 446 nm and 482 nm, respectively. The relative degree of Aβ aggregation was assessed in terms of fluorescence intensity, which was measured by the RF-5300PC spectrofluorophotometer (Shimadzu, Kyoto, Japan). Intensity of each sample was normalized to buffer-only-sample at each time point. Those values were normalized to each 0h-incubation-sample and then the average was calculated.

2-9 Transmission electron microscopy

TEM was performed according to a previously published method (Ono et al. 2008). Each sample (10 μL) was spotted on to a collodion-coated copper grid (NisshinEM, Tokyo, Japan) and incubated for 20 min. The droplet was then displaced with an equal volume of 2% (v/v) glutaraldehyde in water and incubated for an additional 5 min. This solution was wicked off, and the grid was air dried. Samples were examined using the transmission electron microscope H-9500 (Hitachi, Tokyo, Japan).

2-10 Measurement of Ca^{2+} flux

Ca^{2+} flux in CHO-K1 cells was measured using Fluo-4 acetoxymethyl ester (Fluo-4/AM; Dojindo, Kumamoto, Japan). Ca^{2+} flux was induced by 400 nM Aβ or 100 μM nicotine after Aβ incubation. Ca^{2+} response was detected by the Calcium kit-Fluo 4 (Dojindo), according to the manufacturer's instructions. Fluorescence excitation and emission was read at 455 nm and 525 nm, respectively. The change of fluorescence intensity was determined by the Powerscan HT and analyzed by GENE 5 software (Biotek, Tokyo, Japan). All measurement of Ca^{2+} flux experiments were repeated with five individual times and the maximum of Ca^{2+} response peak amplitude at that single time point was chosen for the bar graph. The individual time point at each experiment group was chosen as previous

reports described (Bengtson et al. 2013; Sukumaran et al. 2012), where each maximum of Ca^{2+} reponse peak amplitude exhibited.

2-11 Biochemical assay of protein extracts preparation

To prepare total protein extracts, after washing by PBS buffer, cultured cells were lysed with RIPA buffer (Wako), which contained Complete Protease Inhibitor Cocktail (Roche, Basel, Swizerland). After sonication, samples were centrifuged under the condition of 15,000 rpm, 4˚C, 5 minutes. The supernatant was diluted by 2X sample buffer solution (Wako) with addition of 2-mercaptoethanol and heated under 95˚C for 1 minute. The concentration of proteins was determined using BCA Protein Assay Reagent (Thermo Fisher Scientific K.K., Yokohama, Japan).

2-12 MTS cell proliferation assay

To measure cell viability, H_2O_2 (750μM) was added for 24 hours to induce the cell death and co-incubation with nicotine (0, 10, 100μM) was processed to activate the neuroprotection of CHRNA7. MTS cell proliferation assay was pursued using CellTiter 96® AQueous One Solution Assay (Promega Corporation, Madison, WI, USA), following the manufacturer's instructions. 20μl of CellTiter 96® AQueous One Solution

reagent was added into each well of the 96-well assay plate containing the samples in 100μl of culture medium. The plate was then incubated at 37˚C for 1 hour in a humidified, 5% CO_2 atmosphere. Absorbance at 490nm was recorded using Benchmark Plus Microplate Reader (Bio-Rad Laboratories). All data was normalized to controls, which were under no H_2O_2 addition.

2-13 Fluorescence microscopy

Cellstain®-Double Staining Kit (Dojindo Laboratories, Kumamoto, Japan) was utilized for simultaneous fluorescence staining of viable and dead cells. Calcein-AM solution was used for viable cells and Propidium Iodide (PI) solution used to stain dead cells, observed by EVOS Floid Cell Imaging Station (Life Technologies). The protocol was pursued according to the manufacturer's instructions. The dye solution was made of Calcein-AM 2μmol/l and PI 4μmol/l. Cultured cells were collected by trypsin and centrifuged under the condition of 1000xg, 3 minutes. The cell pellet was then re-dissolved by 200μl PBS and added by 100μl dye solution. 20μl of the sample was dropped onto the slide glass and covered by cover glass. Green (Calcein-AM) and red (PI) fluorescence was detected simultaneously by the excitation of 490nm. Cell number was counted by ImageJ (NIH) manually using cell counter plugin. 5 fields of view were randomly chosen

from each kind of samples, counted, averaged, normalized to the control sample without extra condition to measure the cell viability.

2-14 Statistical analysis

The data in all the experiments were expressed as means ± SD from three to five independent experiments. Data presented from chapter 3-1 to chapter 3-6 were analyzed using Student's t-test, where difference between samples was considered as statistically significant at $p^* < 0.05$, $p^{**} < 0.01$. Statistically significant differences between groups presented from chapter 3-7 to chapter 3-9 were determined by an analysis of variance (ANOVA) followed by a Dunnett's test. The level of statistical significance was taken at $p^* < 0.05$, $p^{**} < 0.01$.

2-15 Dot Blot

Polyvinylidene difluoride membranes (PVDF membrane, Millipore) was pre-wetted for 1 minute in 100% Methanol to allow membrane activation and then soaked in distilled water for 2 minutes followed directly by 5 minutes' equilibration in TBST (20mM Tris, 150 mM NaCl, 0.1% Tween 20 (Biorad, Hercules, CA, USA), pH7,5). Then PVDF membrane was placed on top of filter stack and 10µl of protein is spotted within a pre marked grid.

The membrane is then left to dry to fix the proteins for 1.5 h at room temperature. Nonspecific binding was blocked with 5% skim milk (Wako) containing 0.1% Tween 20 in TBS after overnight incubation of desired Aβ solution within different concentration. Membrane was then incubated with the desired dilution of primary antibody. For the detection, same protocol was used as the detected-part in western blotting. ImageJ (NIH) was used as an automatic image analysis software to do the quantification.

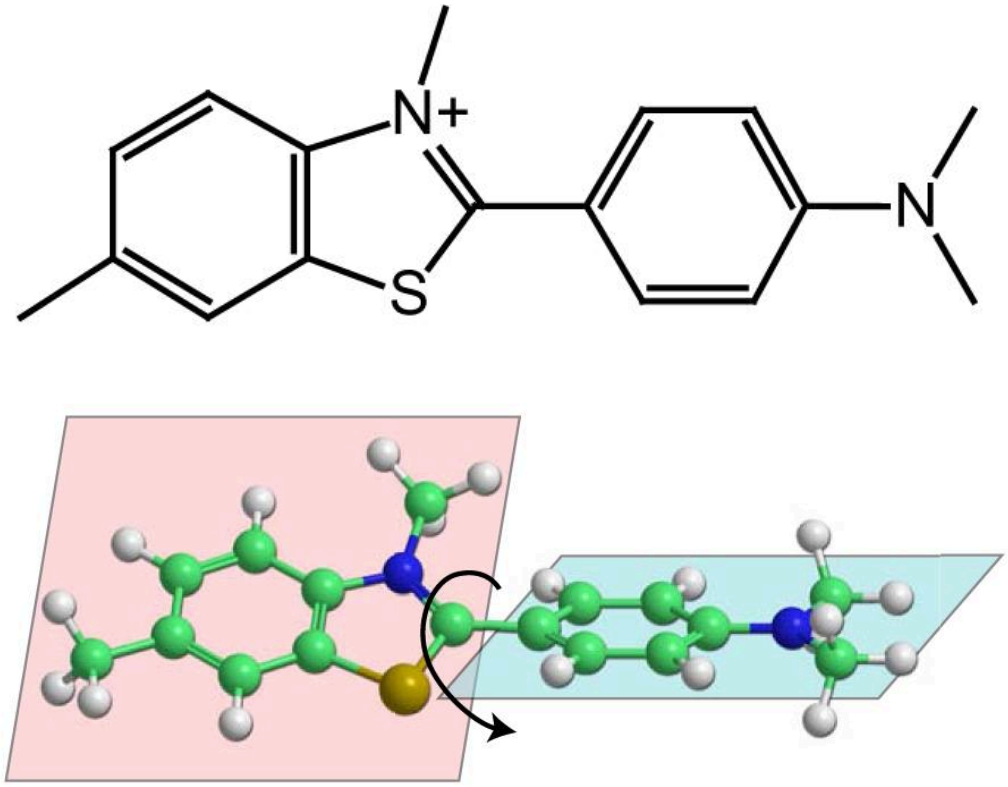

Figure 2-1 ThT structure (cited from Biancalana & Koide 2010)

Structure of ThT (top). The two planer segments of ThT whose mutual rotation defines chirality are also shown (bottom).

Chapter 3 Results

3-1 Arctic Aβ40 specifically bound to CHRNA7

An *in vitro* binding experiment was first performed using several types of synthetic Aβ with GST-CHRNA7. The direct interaction of Dutch, Iowa, and Arctic Aβ40 with CHRNA7 was tested. These mutations have the potential to affect all factors (i.e., the production, degradation, aggregation), known to regulate Aβ monomer levels. As the result, only Arctic Aβ40 bound to CHRNA7 with high affinity (Figure 3-1A). Furthermore, quantification of western blot for Aβ immune reactivity showed that Arctic Aβ40 bound to GST-CHRNA7 with significantly higher affinity than wild-type Aβ40 (**$p<0.01$; Figure 3-1B). As the negative control, an *in vitro* binding experiment was performed using Arctic Aβ40 with GST-CHRNA7 or GST protein. Arctic Aβ did not bound to GST protein (Figure 3-1C), suggesting that GST vector showed lack of the influence on this Arctic Aβ-CHRNA7 interaction.

A. *In vitro* binding: GST-CHRNA7 + Aβ40

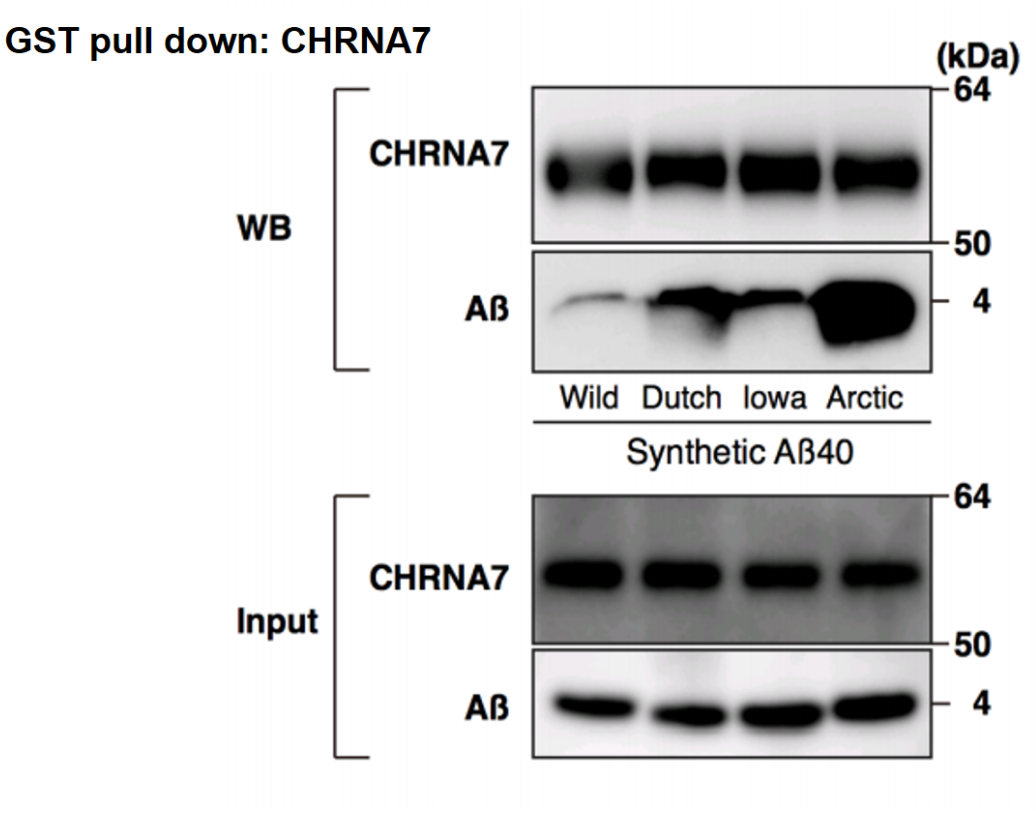

B. Quantification of *in vitro* binding: GST-CHRNA7 + Arctic Aβ

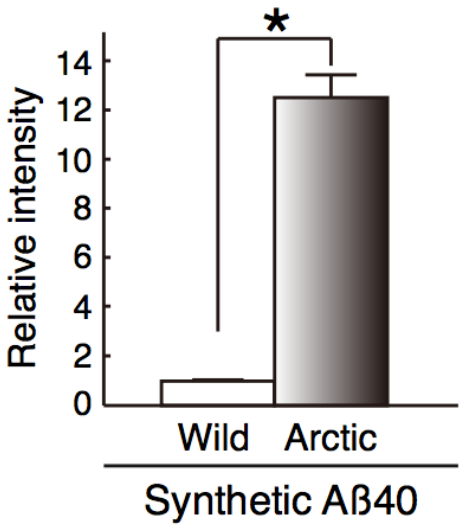

C. *In vitro* binding: GST or GST-CHRNA7 + Arctic Aβ40

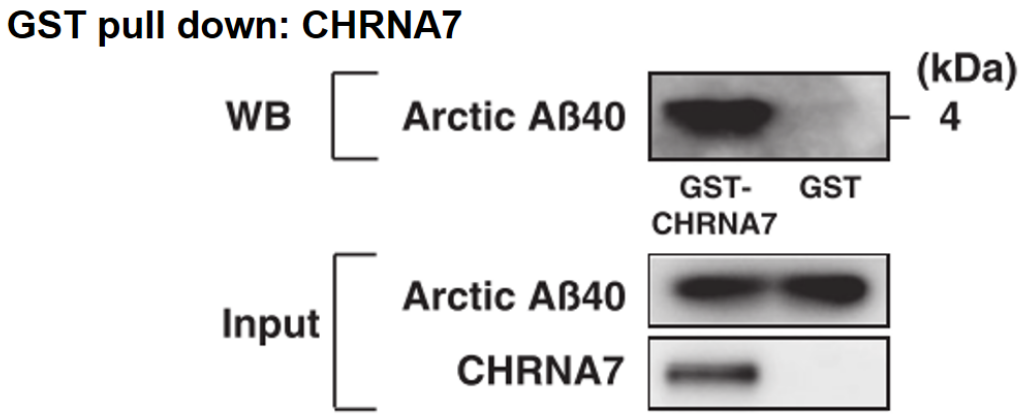

Figure 3-1 Arctic Aβ40 specifically binds to neuronal acetylcholine receptor subunit alpha-7 (CHRNA7) (cited from Ju et al. 2014)

(A) An *in vitro* binding experiment was performed using three types of mutant Aβ that are commonly found in early-onset FAD: Dutch, Iowa, and Arctic Aβ. Only Arctic Aβ40 binds to CHRNA7 with high affinity. (B) Arctic Aβ40 bound to GST-CHRNA7 with significantly higher affinity than wild type Aβ40 (**$p<0.01$). Quantification of western blot for Aβ immunoreactivity is represented as means ± SD (n=3). (C) An *in vitro* binding experiment using Arctic Aβ with GST-CHRNA7 or GST protein was performed. Arctic Aβ binds to GST-CHRNA7 with high affinity. Meanwhile, Arctic Aβ does not bind to GST protein.

3-2 Arctic Aβ42 bound to CHRNA7 with higher affinity than wild-type Aβ42

Aβ42 has been thought to have a stronger association with AD (H. Wang et al. 2000). Therefore, the interaction of wild-type Aβ42 and Arctic Aβ42 with CHRNA7 was tested by *in vitro* binding experiment. As the result, Arctic Aβ42 bound to CHRNA7 more strongly than wild-type Aβ42 (Figure 3-2). However, the bands corresponded to aggregated Aβ42 (~8kDa) was also detectable (Figure 3-2). Since the aggregates bands were visible in the input sample as well (Figure 3-2, arrowhead), it was difficult to clarify whether the interaction between aggregated Aβ42 and CHRNA7 occurred before or after Arctic Aβ42 self-accumulating. Physiological phenomenon of cells can be affected by the accumulation of Arctic Aβ42 itself bypassing or including CHRNA7. Therefore, to exclude the effect of self-aggregation of Arctic Aβ in order to focus on the effect of the mutant Aβ on CHRNA7, Arctic Aβ1-40 peptides were utilized, which did not show self-aggregation in experimental conditions (Figure 3-1), to do the further research.

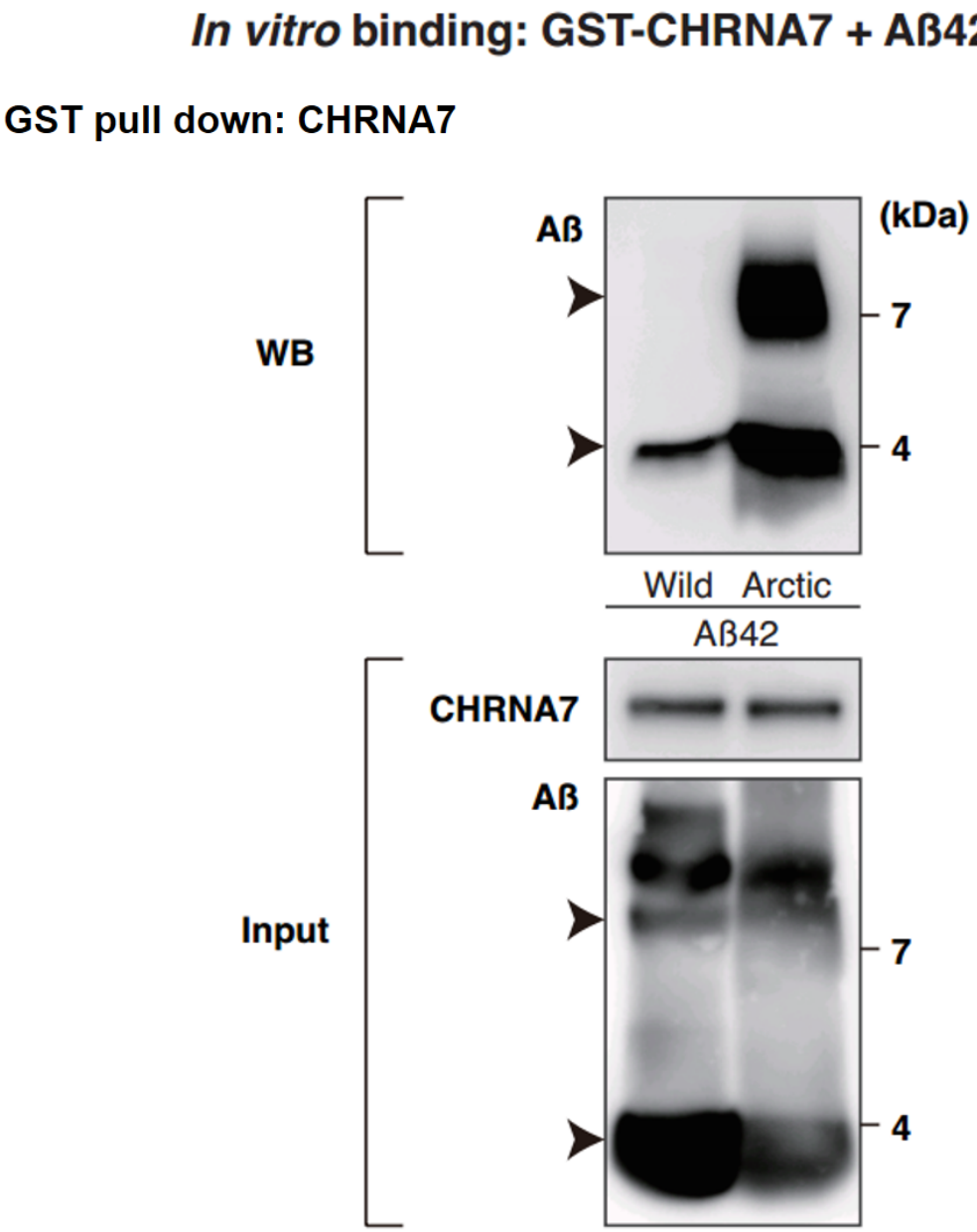

Figure 3-2 Arctic Aβ42 bound to CHRNA7 with higher affinity than wild type (cited from Ju et al. 2014)

An *in vitro* binding experiment using Arctic Aβ42 and wild type Aβ42 was performed. Arctic Aβ42 binds to CHRNA7 more strongly than wild type Aβ42

while the bands corresponded to Aβ42 dimer (~8kDa) is also detectable. Aggregates are visible in input sample used for *in vitro* binding experiment as well (arrow showed), suggesting the self-accumulation of Arctic Aβ42 and wild-type Aβ42.

3-3 Arctic Aβ enhanced its aggregation with the incubation of CHRNA7

The Arctic mutation has been reported to induce a rapid formation of protofibrils, thus leading to an alternative pathogenic mechanism for FAD (Nilsberth et al. 2001). Fibril formation by the Arctic mutation has also been found under both *in vitro* (Murakami et al. 2003) and *in vivo* (Cheng et al. 2007) conditions.

In the present study, the aggregation form of Arctic Aβ affected by CHRNA7 was investigated via ThT assay and TEM. The ThT assay showed that Arctic Aβ started to aggregate at 6h when co-incubated with CHRNA7. Arctic Aβ alone itself did not aggregate at this time point (Figure 3-3B). Furthermore, Arctic Aβ enhanced the aggregation at 9h when co-incubated with CHRNA7, significantly greater than Arctic Aβ alone itself (Figure 3-3B). Meanwhile, wild-type Aβ40 did not aggregate with or without the co-incubation with CHRNA7 (Figure 3-3A).

The same phenomenon was observed via TEM as well. Accumulation of Arctic Aβ was quite clear when co-incubated with CHRNA7 for 24h compared with Arctic Aβ alone (Figure 3-4). A and B, C and D described different fields of view within 2 kinds of samples. As a result, aggregation of Arctic Aβ was enhanced with the addition of CHRNA7.

A. ThT assay of Aβ40 with or without CHNRA7

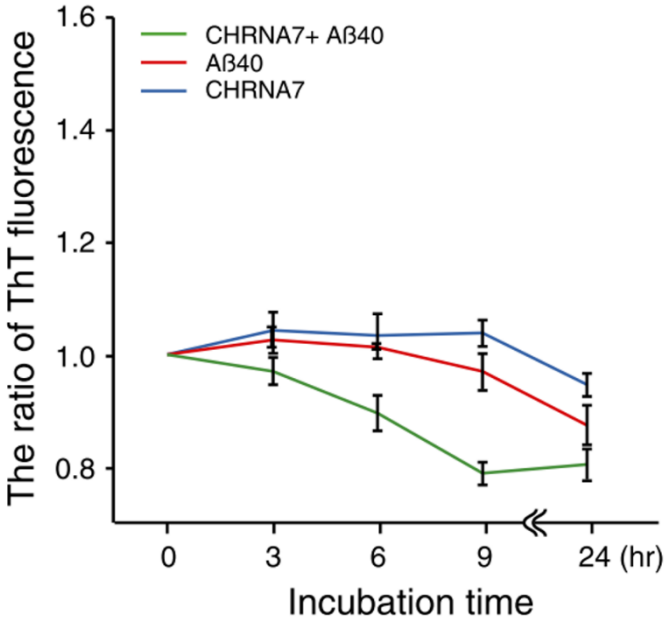

B. ThT assay of Arctic Aβ40 with or without CHNRA7

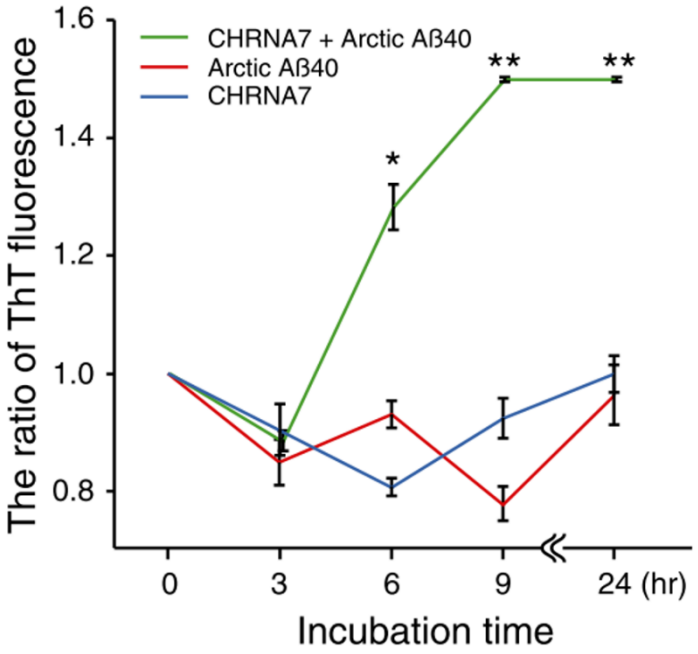

Figure 3-3 Arctic Aβ enhanced its aggregation with addition of CHRNA7 detected by Thioflavin T (ThT) assay (cited from Ju et al. 2014)

The ThT assay was used to determine the aggregation form in presence of CHRNA7 over time. (A) Wild-type Aβ40 does not aggregate when co-incubated with CHRNA7; (B) Compare with Arctic Aβ alone, the addition of CHRNA7 helps Arctic Aβ aggregates further (*$p<0.05$ at the time point of 6h, **$p<0.01$ at the time point of 9h, 24h). The data of each time point is represented as means ± SD (n=3).

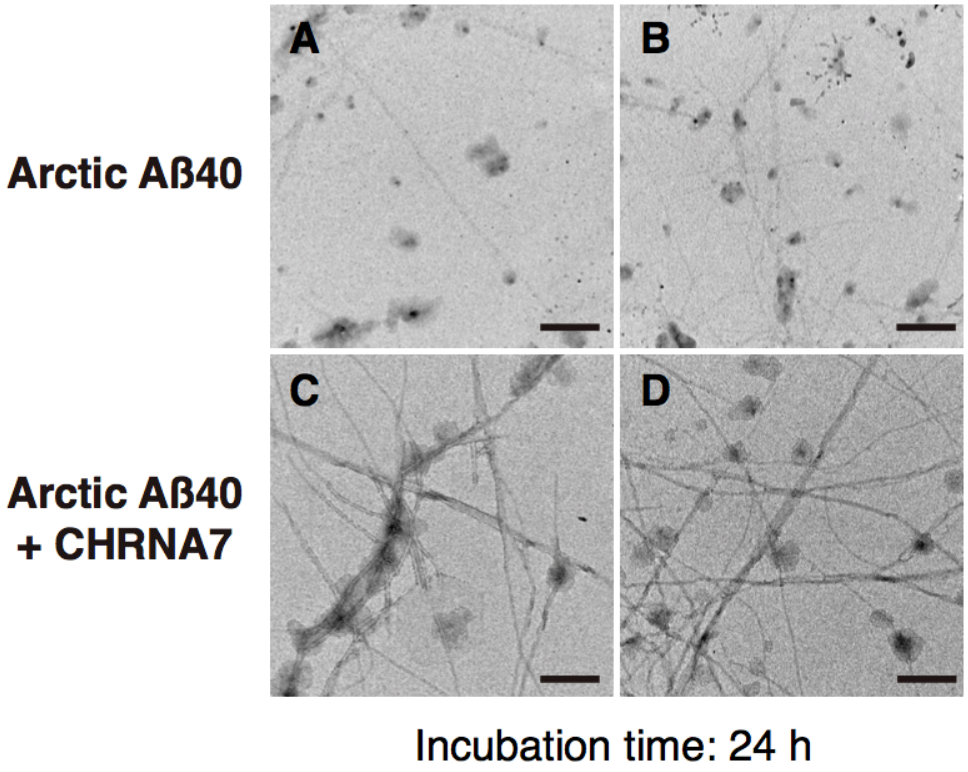

Figure 3-4 Arctic Aβ enhanced its aggregation with addition of CHRNA7 observed by Transmission electron microscopy (TEM) (cited from Ju et al. 2014)

Synthetic Arctic Aβ incubated at 37˚C for 24 hours, with or without CHRNA7, then observed by TEM. Arctic Aβ clearly accumulates when co-incubated with CHRNA7 (panel C, D). However, the aggregation phenomenon in Arctic Aβ alone sample is not as significantly visible as the Arctic Aβ-CHRNA7 co-incubation sample (panel A, B) (scale bar = 500nm).

3-4 Arctic Aβ did not modify the function of CHRNA7

CHRNA7 has a high relative permeability to Ca^{2+} and regulates numerous Ca^{2+}-dependent events (Bertrand et al. 1993; Liu et al. 2001; Séguéla et al. 1993). In order to search the effect of Arctic Aβ on the function of CHRNA7, I investigated the Ca^{2+} response and Ca^{2+}-downstream signaling activation of ERK1/2 using the protocol as Figure 3-5 described. The over-expression of CHRNA7 in CHO-K1 cells was confirmed by western blot analysis. CHRNA7 was detected by both anti-HA tag and anti-CHRNA7 antibodies (Figure 3-6). Synthetic Aβ (400nM) was used to determine whether Arctic Aβ induces Ca^{2+} response. As a result, CHO-K1 cells produced a rapid and sharp increase in Ca^{2+} response to Aβ42 (Figure 3-7), confirming a previous report (Dineley et al. 2002). This increase was not seen when Arctic Aβ was added (Figure 3-7). This result leads to a speculation that although Arctic Aβ40 bound to CHRNA7 similarly as Aβ42, Ca^{2+} flux was not the same (Figure 3-7).

Aβ42 was reported to activate MAP kinase cascade via CHRNA7 (Dineley et al. 2001). Thus, the activation of ERK1/2 was examined, as the further test of a downstream Ca^{2+}-dependent event through CHRNA7. The results showed that the addition of Arctic mutant Aβ did not activate ERK1/2 (Figure 3-8).

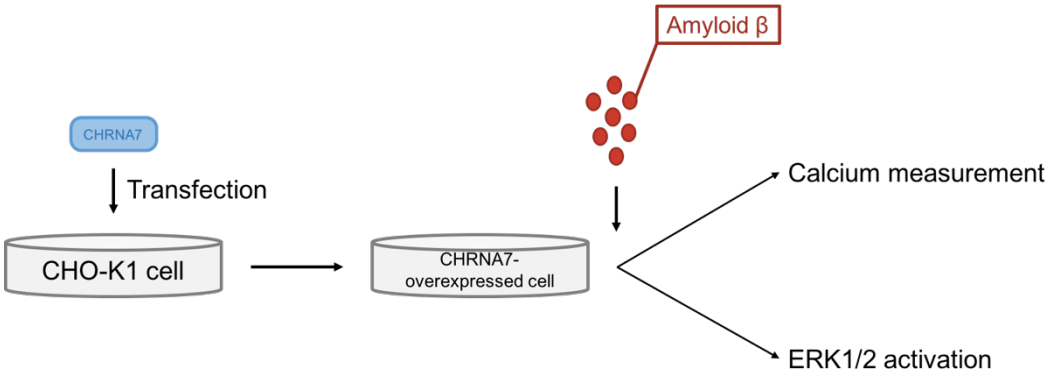

Figure 3-5 Protocol of measuring CHRNA7 functions influenced by Amyloid β

In order to search the effect of Arctic Aβ on the function of CHRNA7, I investigated the Ca^{2+} response and Ca^{2+} -downstream signaling activation of ERK1/2. Synthetic Aβ (400nM) was added into CHRNA - overexpressed CHO-K1 cells. Calcium was measured before and after the immediate addition of Aβ in order to determine whether Arctic Aβ induces Ca^{2+} response. 10 minutes-incubation of Aβ was used to activate ERK1/2, investigating whether Arctic Aβ affects ERK1/2 activation.

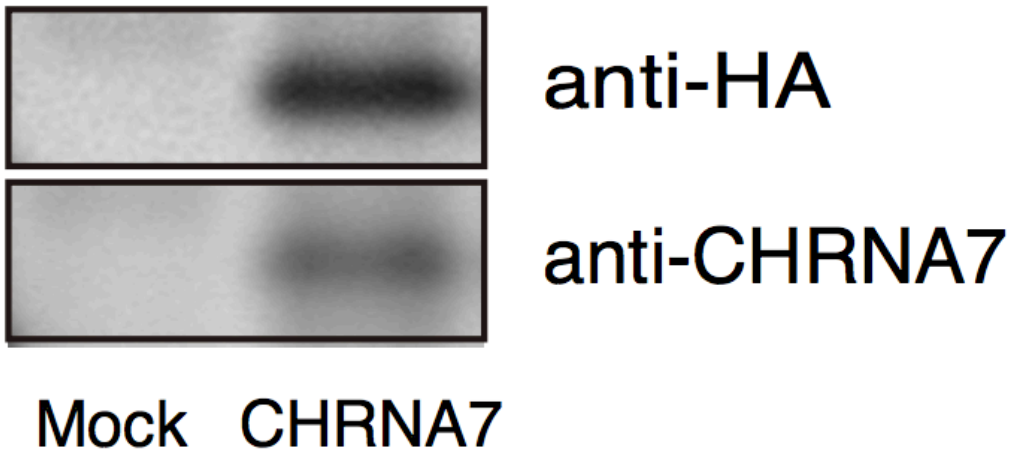

Figure 3-6 Confirmation of the over-expression of CHRNA7 in CHO-K1 cells (cited from Ju et al. 2014)

CHRNA7 expression was confirmed by western blotting. CHRNA7 was detected by anti-HA tag antibody (Medical & Biological laboratories), and anti-CHRNA7 antibody (Santa Cruz Biotechnology). The band observed in CHRNA7-transfected cells was not detectable in lysates from mock-transfected cells.

A. Measurement of Ca^{2+} flux with the addition of Aβ

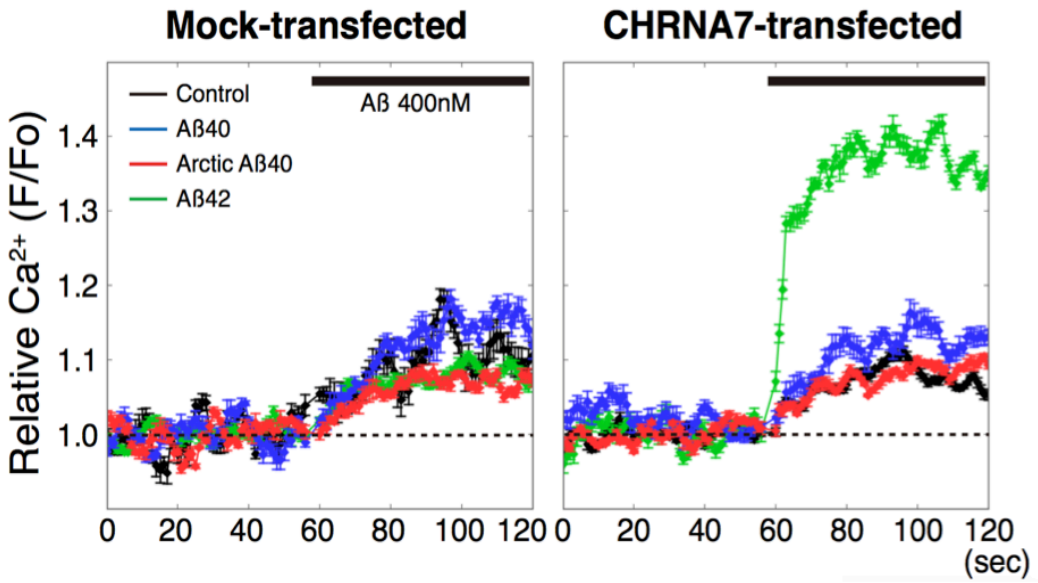

B. Amplitude of Ca^{2+} with the addition of Aβ

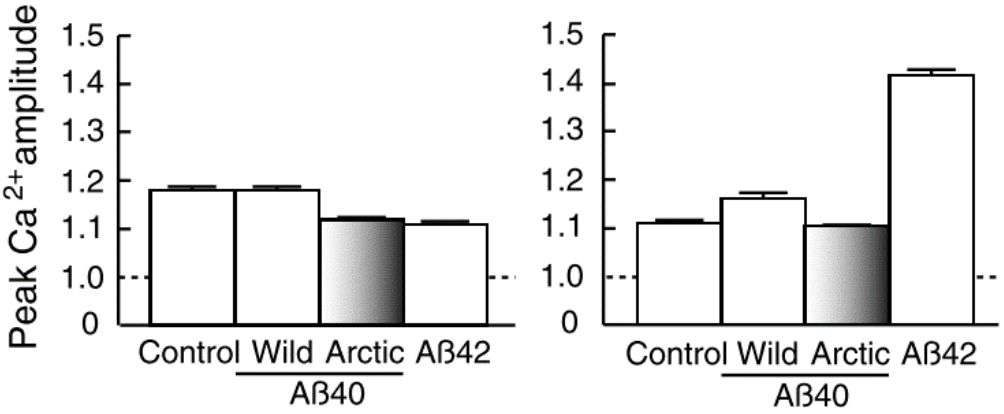

Figure 3-7 Addition of Arctic Aβ does not induce Ca^{2+} responses (cited from Ju et al. 2014)

CHRNA7 was transfected into CHO-K1 cells. (A) Ca^{2+} response to synthetic Aβ was measured using Calcium Kit-Fluo 4 and all measurement of Ca^{2+}

flux experiments was repeated with 5 times. (B) The maximum of Ca^{2+} response peak amplitude at that single time point was chosen for the bar graph and represented as means ± SD (n=5). The results show that Arctic Aβ does not induce Ca^{2+} flux.

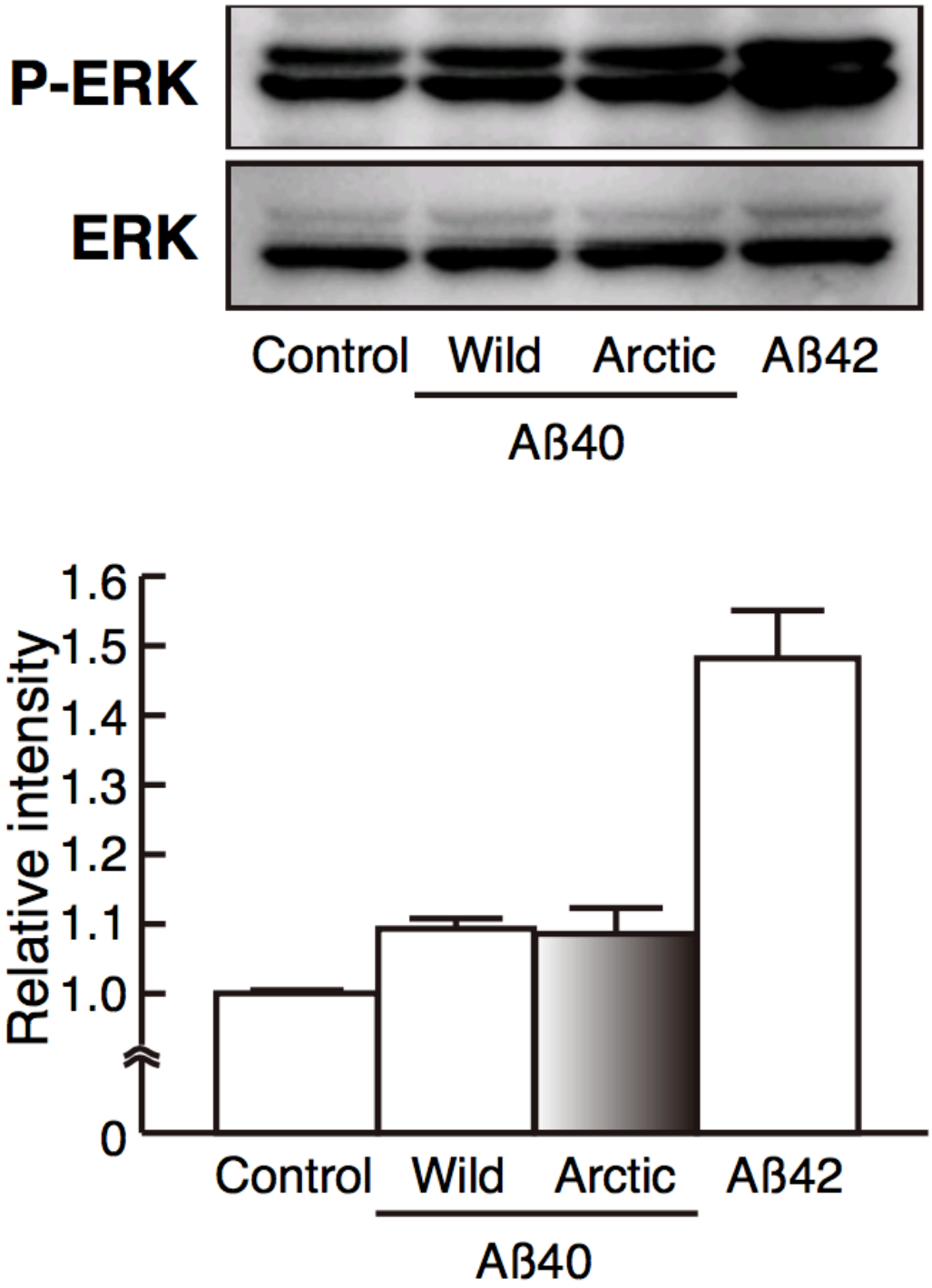

Figure 3-8 Addition of Arctic Aβ does not activate ERK1/2 (cited from Ju et al. 2014)

Synthetic Aβ was added to CHRNA7-overexpressed CHO-K1 cells. Then proteins were extracted and detected by the phospho-p44/42 MAPK (ERK1/2) antibody (Cell Signaling Technology). Quantification of western blot for phospho-ERK1/2 immunoreactivity is represented as means ± SD (n=3).

3-5 Incubated Arctic Aβ inhibited the function of CHRNA7

Since Arctic Aβ enhanced its aggregation when co-incubated with CHRNA7 (chapter 3-3, Figure 3-3; 3-4), the effect of the incubated Arctic Aβ on the function of CHRNA7 was searched. Nicotine was used to activate the Ca^{2+} response after 24-h incubation of Aβ (Figure 3-9). Ca^{2+} response was not induced by nicotine in mock-transfected CHO-K1 cells. Ca^{2+} rapidly increased after the addition of nicotine in CHRNA7-over-expressed-CHO-K1 cells. However, this response was significantly (*$p<0.05$) reduced within the cells incubated with Arctic Aβ40. Therefore, Arctic Aβ tended to attenuate Ca^{2+} response in addition to enhanced its aggregation when co-incubated with CHRNA7 (Figure 3-10).

Furthermore, the activation of ERK1/2, Ca^{2+} - downstream signaling protein, was investigated as a further test of one of the Ca^{2+} - dependent events. The results showed that the incubation of Arctic mutant Aβ actually inhibited the activation of ERK1/2 (Figure 3-11). In short, these results indicated that Arctic Aβ aggregated in the presence of CHRNA7, and suppressed the function of CHRNA7 via the inhibition of Ca^{2+} flux and activation of ERK1/2.

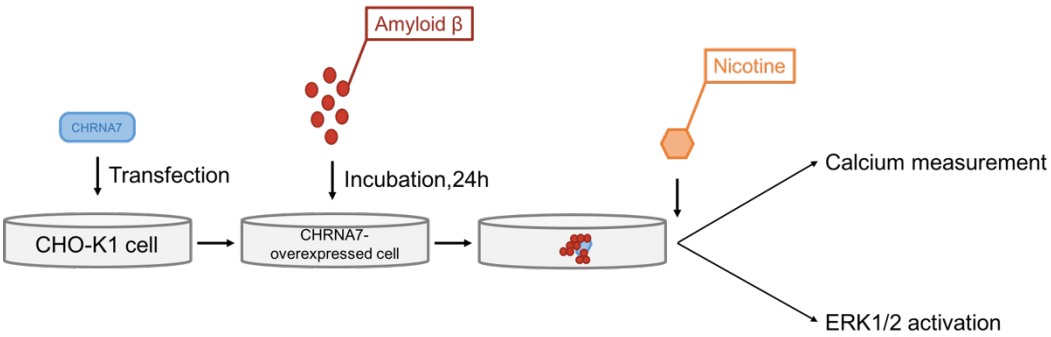

Figure 3-9 Protocol of investigating the influence of incubated Amyloid β on CHNRA7 functions

In order to search the effect of Arctic Aβ incubation on the function of CHRNA7, I investigated the Ca^{2+} response and Ca^{2+} -downstream signaling activation of ERK1/2. Synthetic Aβ (400nM) was added into CHRNA–over-expressed CHO-K1 cells, incubated for 24 hours to aggregate based on the results we gained from chapter 3-3. Calcium was measured before and after the immediate addition of nicotine (100μM). 10 minutes-incubation of nicotine was used to activate ERK1/2, searching whether incubated Arctic Aβ affects ERK1/2 activation.

A. Measurement of Ca^{2+} flux with the incubation of Aβ

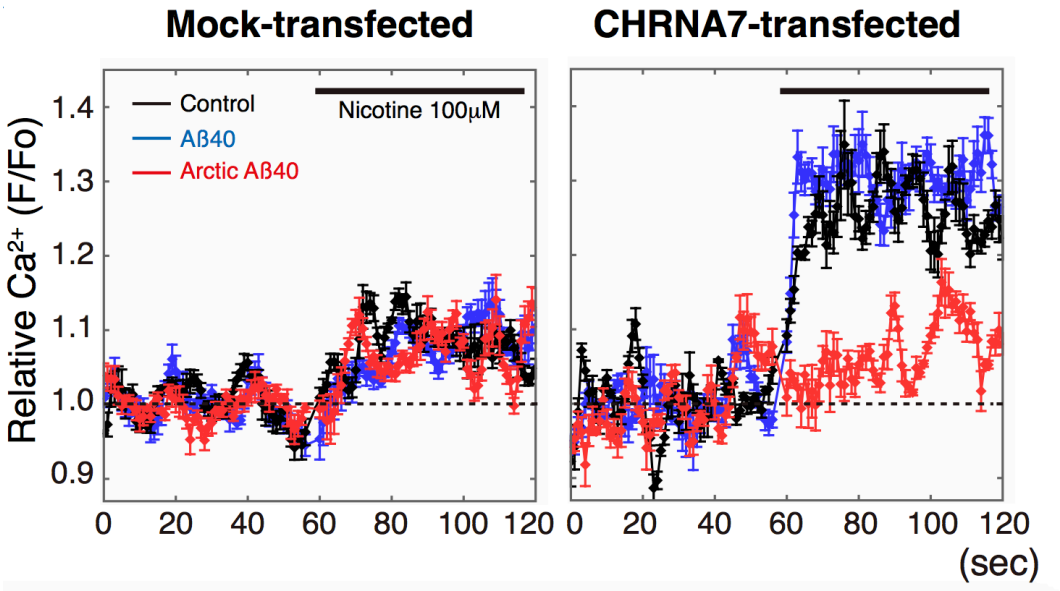

B. Amplitude of Ca^{2+} with the incubation of Aβ

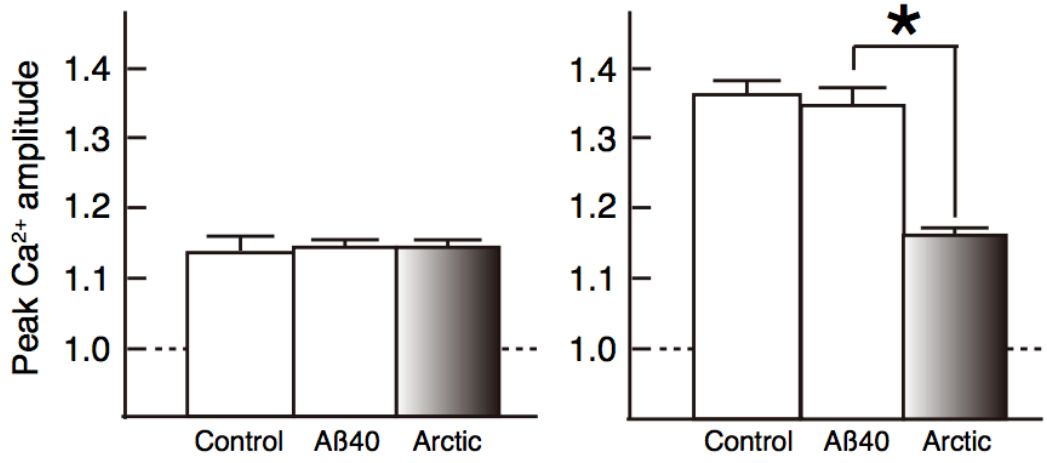

Figure 3-10 Incubated Arctic Aβ inhibits the Ca^{2+} response via CHRNA7 (cited from Ju et al. 2014)

CHRNA7 was transfected into CHO-K1 cells. Nicotine was used to activate CHNRA7 after 1-day incubation with or without Aβ (n=5). (A) Cells with Arctic Aβ40 incubation significantly diminished the Ca^{2+} response (*$p<0.05$). (B) The maximum of Ca^{2+} response peak amplitude at that single time point was chosen for the bar graph and represented as means ± SD (n=5).

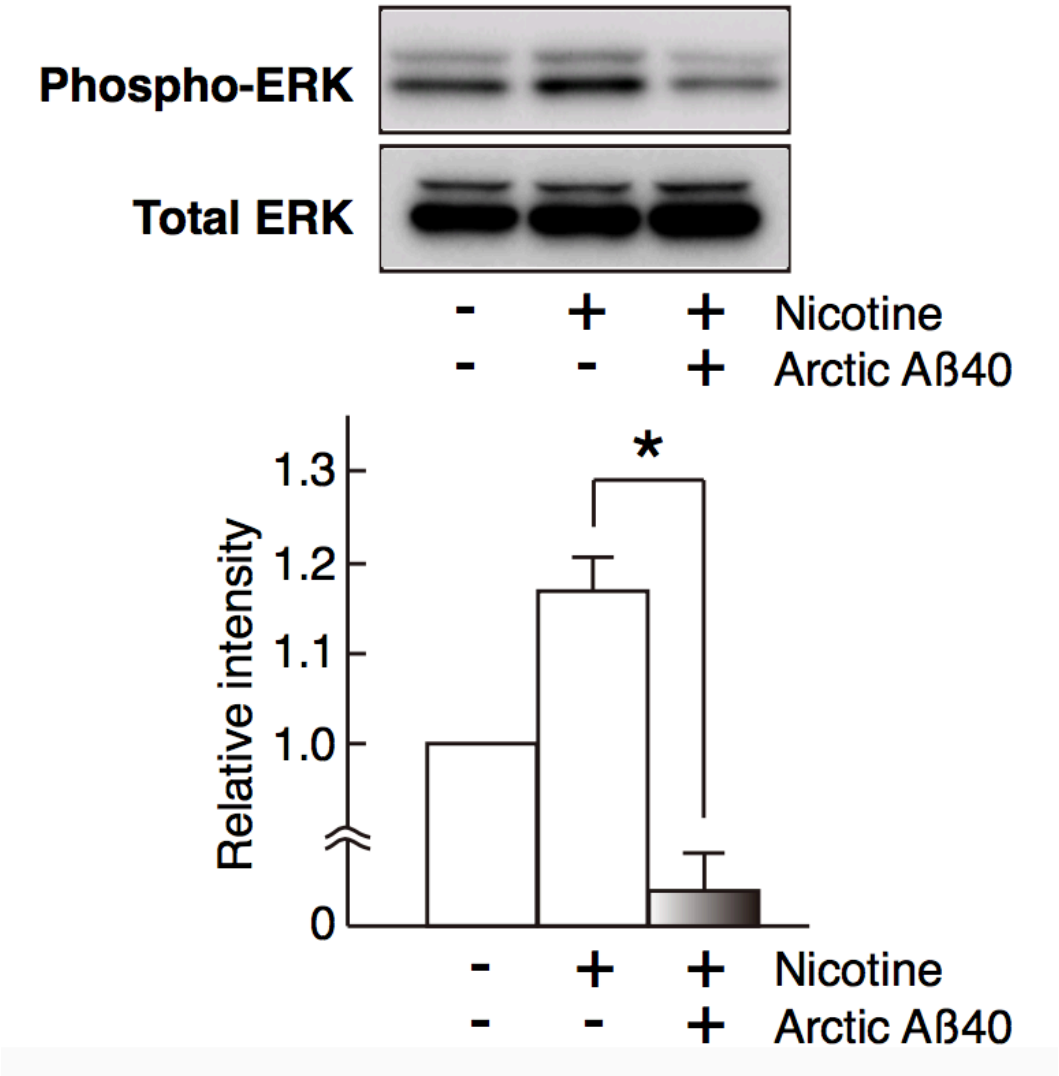

Figure 3-11 Incubated Arctic Aβ inhibits the activation of ERK1/2 (cited from Ju et al. 2014)

CHRNA7 was transfected into CHO-K1 cells and synthetic Aβ was added after 24 hours, incubated for 1 day. After activation of CHRNA7 by nicotine for 10 minutes, proteins were extracted and detected by the phospho-p44/42 MAPK (ERK1/2) antibody (Cell Signaling Technology).

Quantification of western blot for phospho-ERK1/2 immunoreactivity is represented as means ± SD (n=3).

3-6 Neuroprotective effect of CHRNA7 by nicotine was blocked by the knockdown of CHRNA7

The contents from 3-6 to 3-8 is under review of the scientific journal. CHRNA7 was reported to have neuroprotective function against oxidative stress through multiple pathway but not confirmed (Guan et al. 2001; Qi et al. 2013; Javier Egea et al. 2007). Arctic mutation-mediated FAD has been reported the increased oxidative stress as well (Ronnback et al. 2016). In order to search the neuroprotective function of CHRNA7, Hydrogen peroxide (H_2O_2) was applied as an oxidative stress inducer (Wang et al. 2003) and nicotine as to activate CHRNA7 (Dajas-Bailador et al. 2000; Iwamoto et al. 2013; Shin et al. 2007) in this study's experiments. Both retinoic acid (RA) differentiated (Cavanaugh et al. 2006; Fernandez-Gomez et al. 2006) and un-differentiated SH-SY5Y cells (Xue et al. 2006; Levites et al. 2002) have been used in neuroscience research as an *in vitro* model for neurotoxity experiment (Cheung et al. 2009), therefore, in this study neuronal cell model SH-SY5Y human neuroblastoma cells were utilized.

RNA interference (RNAi) was used to knock down the expression of CHRNA7, so that the neuroprotective function of CHRNA7 against oxidative stress activated by nicotine could be confirmed. I transfected the shRNA vector (1, 2, scramble) of CHRNA7 and CHRNA7-contained vector into SH-SY5Y cells simultaneously. Cells without shRNA vector transfected were

utilized as control. H_2O_2 (750μM) was added for 24 hours to induce the cell death and co-incubation with nicotine (0, 10, 100μM) was processed to activate the neuroprotective function of CHRNA7.

Cells transfected with scramble shRNA expressed the similar levels of CHRNA7 as the cells without RNAi transfected, confirming that scramble shRNA did not target any endogenous transcript and could be employed to control for non-specific effects (Figure 3-12). Comparing with the control sample, cells transfected with shRNA expressed the decreases in the levels of CHRNA7 protein (Figure 3-12). The neuroprotective function of CHRNA7 against oxidative stress activated by nicotine was confirmed (Figure 3-13, no RNAi and scramble). However, with the knock-down of CHRNA7 using RNAi, nicotine failed to rescue the cell-death from oxidative stress (Figure 3-13, RNAi-1 and RNAi-2). The results confirmed that neuroprotective function against oxidative stress was mediated through CHRNA7 activated by nicotine, because this neuroprotective function was blocked by the knock-down of CHRNA7 through RNAi.

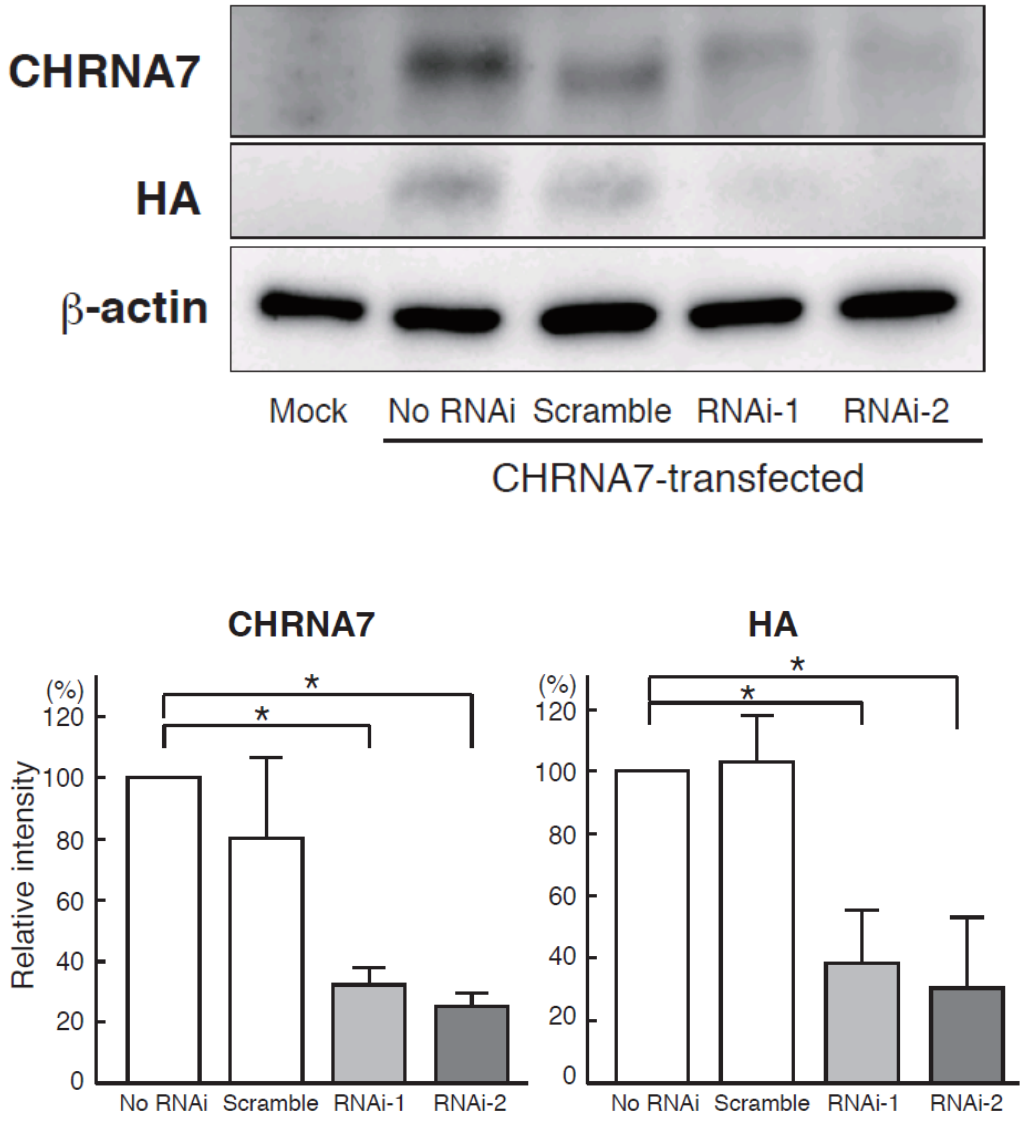

Figure 3-12 Decreased expression of CHRNA7 using RNAi

CHRNA7 vector and shRNA vectors were co-transfected into SH-SY5Y cells. Cells transfected with scramble shRNA expressed the similar levels of CHRNA7 as the cells without RNAi transfected. Compared with the control sample, cells transfected with RNAi-1 and RNAi-2 express the

decreases in the levels of CHRNA7 protein significantly (*p<0.05). Quantification of western blot is represented as means ± SD (n=3).

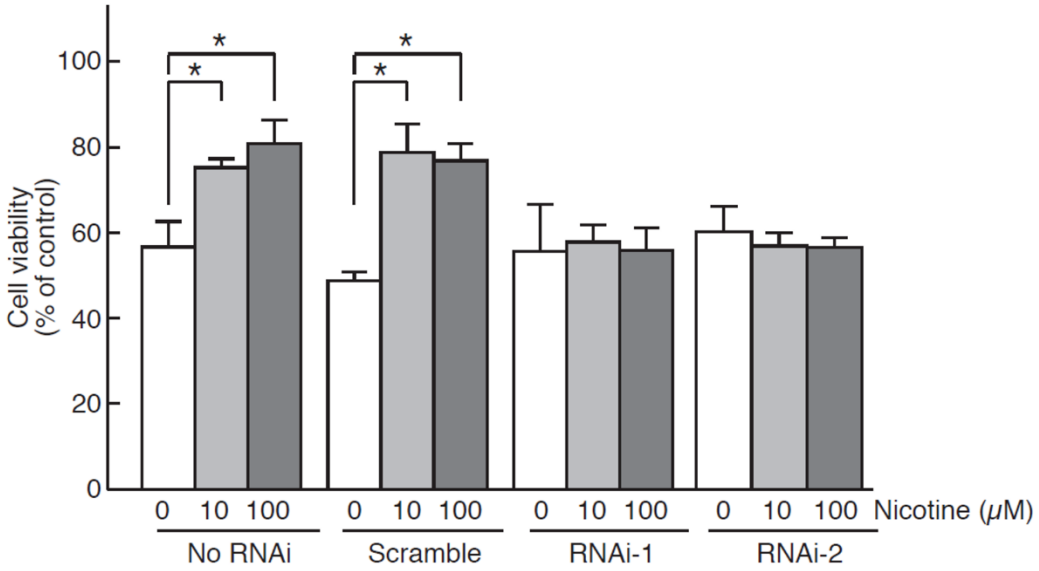

Figure 3-13 Neuroprotective effect of CHRNA7 activated by nicotine was blocked by the knockdown of CHRNA7

CHRNA7 has the neuroprotective function against oxidative stress activated by nicotine (no RNAi and scramble shRNA transfected; *$p<0.05$). Nicotine shows no effect on the neuroprotection of cell viability by MTS assay with the knock-down of CHRNA7 using RNAi (RNAi-1 and RNAi-2). Quantification of the MTS assay is represented as means ± SD (n=3).

3-7 Arctic Aβ inhibited the nicotine activated neuroprotective functions through CHRNA7

Previous results suggested that immediate Arctic Aβ addition did not modify the function of CHRNA7 (Ju et al. 2014). Meanwhile, co-incubation with Arctic Aβ successfully inhibited the functions of CHRNA7 (Ju et al. 2014). In this study, SH-SY5Y cells was utilized to investigate whether Arctic Aβ affects the neuroprotective function of CHRNA7 activated by nicotine. Following the protocol described in Figure 3-14, over-expressed CHRNA7 into SH-SY5Y cells and incubated Arctic Aβ or wild-type Aβ (400nM) for 24 hours. H_2O_2 (750μM) was then added for 24 hours to induce the cell death and co-incubation with nicotine (0, 10, 100μM) was processed to promote the neuroprotective effect (Figure 3-14). From the results from MTS cell proliferation assay, I noticed that the incubation of Arctic Aβ significantly inhibited the neuroprotective function activated by nicotine ($p^* < 0.05$, Figure 3-15A). Furthermore, wild-type Aβ40 showed no influence on this effect (Figure 3-15A), suggesting that the mutation of Aβ played the critical role in affecting this interference, but not Aβ peptide itself.

To exclude the influence of endogenous CHRNA7 and other unrelated channels in SH-SY5Y cells, the same experiment was performed using the mock-transfected cells. The result showed that endogenous CHRNA7 in SH-SY5Y cells was not enough to present its own neuroprotective function

activated by nicotine (Figure 3-15B). In this case, both Arctic and wild-type Aβ had no influence on rescue nor enhance the cell-death caused by oxidative stress (Figure 3-15B).

The similar phenomenon was also observed via fluorescence microscopy. I stained the viable and dead cells simultaneously by Calcein-AM solution and Propidium Iodide (PI) solution (Figure 3-16A). In order to dye the cells uniformly and count the cells easily, cultured cells were collected by trypsin and centrifuged, cell pellet then re-dissolved and dropped onto the slide glass to be dispersed (Figure 3-16A). Nicotine was found to rescue the cell-death form oxidative stress caused by H_2O_2, by activating the CHRNA7, which was over-expressed into SH-SY5Y cells (Figure 3-16). Arctic Aβ significantly ($*p < 0.05$) inhibited the nicotine-activated neuroprotective function through CHRNA7 (Figure 3-15, 3-16).

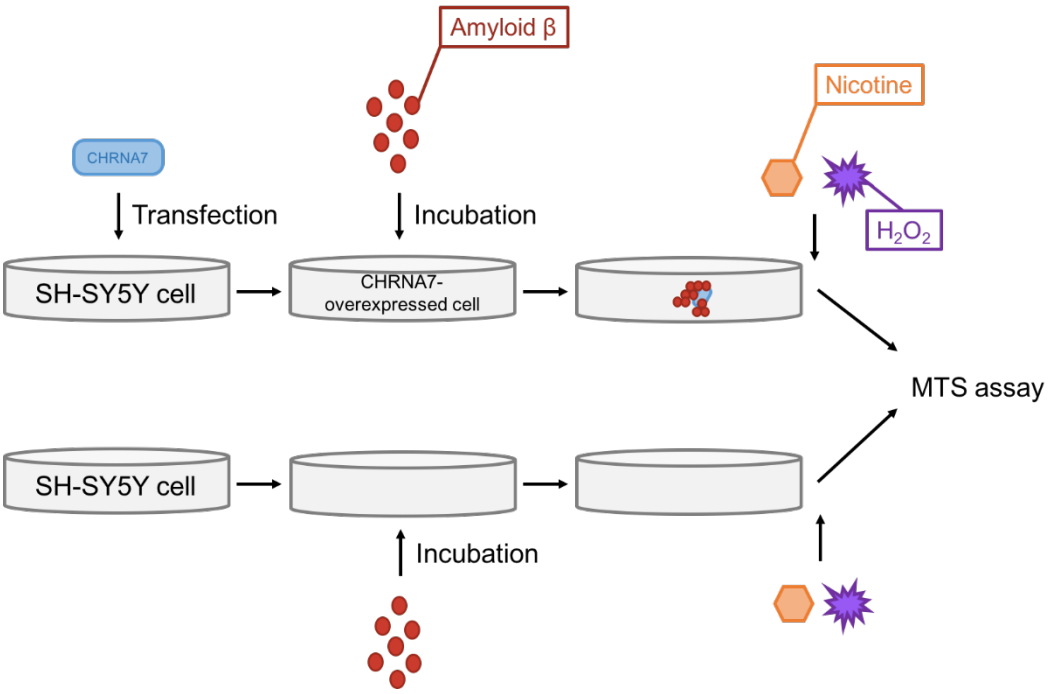

Figure 3-14 Protocol of measuring neuroprotection of CHRNA7 affected by incubated Amyloid β

In order to search neuroprotection of CHRNA7, MTS assay was used to measure the cell viability. CHRNA7 was over-expressed into SH-SY5Y cells and Arctic Aβ or wild-type Aβ (400nM) was added after one day, incubated for 24 hours. H_2O_2 (750μM) was added for 24 hours to induce the cell death and co-incubation with nicotine (0, 10, 100μM) was processed to promote the neuroprotective effect.

A. CHRNA7 transfected SH-SY5Y cells

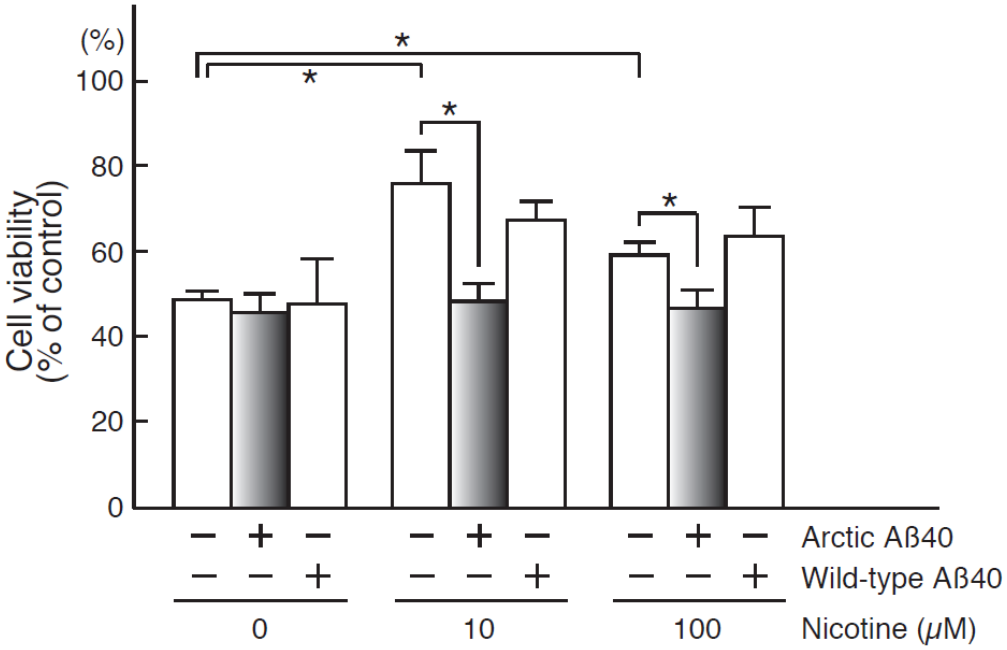

B. Mock-transfected SH-SY5Y cells

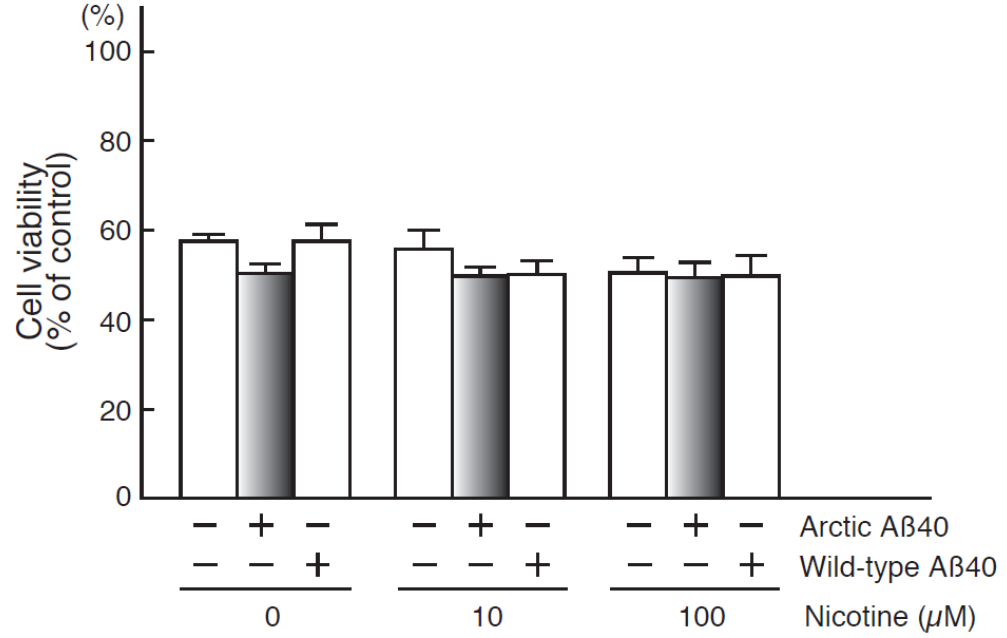

Figure 3-15 Arctic Aβ inhibits neuroprotective functions through CHRNA7 by MTS cell proliferation assay

(A) CHRNA7 was transfected into SH-SY5Y cells and Arctic or wild-type Aβ40 (400nM) was added after 24h. After one-day incubation, H_2O_2 (750μM) was added for 24 hours to induce the cell death. Addition of nicotine (0, 10, 100μM) was processed to activate the anti-apoptotic effect by activating CHRNA7. Incubated Arctic Aβ significantly inhibits the neuroprotective function activated by nicotine ($*p < 0.05$). Wild-type Aβ40 shows no influence on this effect. Quantification of the MTS assay is represented as means ± SD (n=3). (B) Mock-transfect SH-SY5Y cells were utilized. As a result, Arctic and wild-type Aβ both has no influence on rescue or enhance the cell-death caused by oxidative stress. This indicates that endogenous CHRNA7 or other unrelated channels in SH-SY5Y cells are not enough to present the nicotine-induced neuroprotective function through CHNRA7.

A

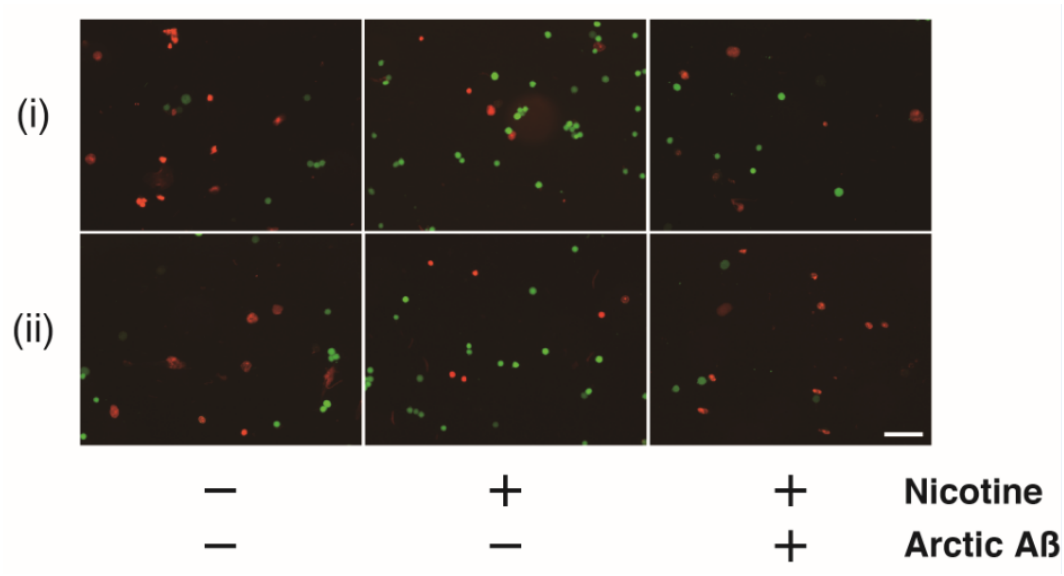

B

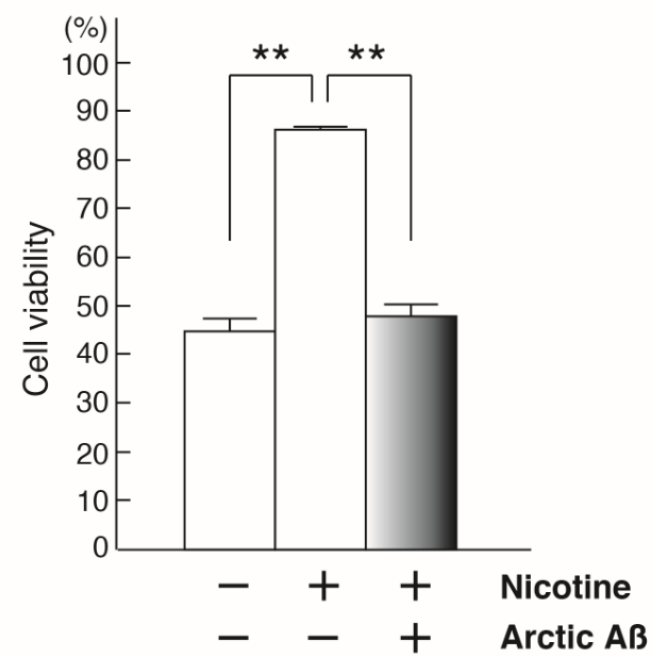

Figure 3-16 Arctic Aβ inhibits neuroprotective functions through CHRNA7 by fluorescence microscopy

CHRNA7 was transfected into SH-SY5Y cells. (A) Viable cells are stained by Calcein-AM solution (green) and dead cells are stained by Propidium Iodide (PI) solution (red) simultaneously (scale bar = 100μM). In order to dye the cells uniformly and count the cells easily, cultured cells were collected by trypsin and centrifuged, cell pellet then re-dissolved and dropped on to the slide glass to be dispersed. i, ii described different fields of view within 3 kinds of samples. (B) Incubated Arctic Aβ significantly (**$p < 0.01$) inhibits nicotine-mediated neuroprotective function of CHRNA7 against oxidative stress. Quantification of fluorescence microscopy represents means ± SD (n=3).

3-8 Activation of ERK1/2 was the key signaling protein participating in Arctic Aβ-mediated-interference on neuroprotective function

Previous study described that the addition of incubated Arctic mutant Aβ inhibited the activation of ERK1/2 in non-neuronal CHO-K1 cells (Ju et al. 2014). There were several different signaling cascades (i.e. ERK1/2 (Toborek et al. 2007; Ren et al. 2005), JNK (Huang et al. 2012), and AKT pathway (Kihara et al. 2001; Buckinham et al. 2009)) reported to be participating in neuronal cell survival within nicotine anti-apoptotic actions. Therefore, here I investigated the activation of other signaling proteins as well as ERK1/2 to search which kinds of signaling proteins were participating in the Arctic Aβ-mediated-effect on functions of CHRNA7 activated by nicotine in neuronal SH-SY5Y cells. As the result, addition of the Arctic Aβ only inhibited the activation of ERK1/2 but no other signaling proteins (Figure 3-17A). This effect was performed by CHRNA7 because those cells without over-expressed CHRNA7 showed none of the activation change of signaling proteins (Figure 3-17B). This result suggested that ERK1/2 was the key signaling protein participating in Arctic Aβ-mediated-interference on functions of CHRNA7 activated by nicotine in neuronal cells.

In order to further test whether the activation of ERK1/2 is mediating the nicotine effect in neuroprotection against oxidative stress induced by H_2O_2,

SH-SY5Y cells was treated with PD98059, which served as a specific inhibitor of MAPK extracellular signaling-regulated kinase (ERK) kinase (MEK) (Hotokezaka et al. 2002). After over-expressing CHRNA7 in SH-SY5Y cells, 5μM and 50μM PD98059 was added for one hour prior to treating with nicotine to activate ERK1/2. As the result, both 5μM and 50μM PD98059 significantly inhibited the activation of ERK1/2, while 50μM clearly inhibited further (*$p<0.05$, **$p<0.01$, Figure 3-18A). However, cells pretreated with 50μM PD98059 appeared to have more toxicity, that cells were mostly dead before adding H_2O_2 and nicotine to measure cell viability (data not shown). Therefore, cells pretreated with 5μM PD98059 were used to measure the cell viability. H_2O_2 (750μM) was added for 24 hours to induce the cell death and addition of nicotine was processed to activate the neuroprotective effect by activating CHRNA7. In CHRNA7-transfected cells, treatment of PD98059 significantly blocked the neuroprotective effect against oxidative stress (*$p<0.05$, Figure 3-18B). This result suggested ERK1/2 at the MEK level efficiently blocked nicotine-mediated protection against oxidative stress induced by H_2O_2. Mock-transfected cells failed to show the nicotine-induced neuroprotection, which excluded the influence of endogenous CHRNA7 in SH-SY5Y cells (Figure 3-18B). Combine together, these results supported that activation of ERK1/2 is mediating the nicotine effect in neuroprotection against oxidative stress induced by H_2O_2.

A. CHRNA7 transfected SH-SY5Y cells

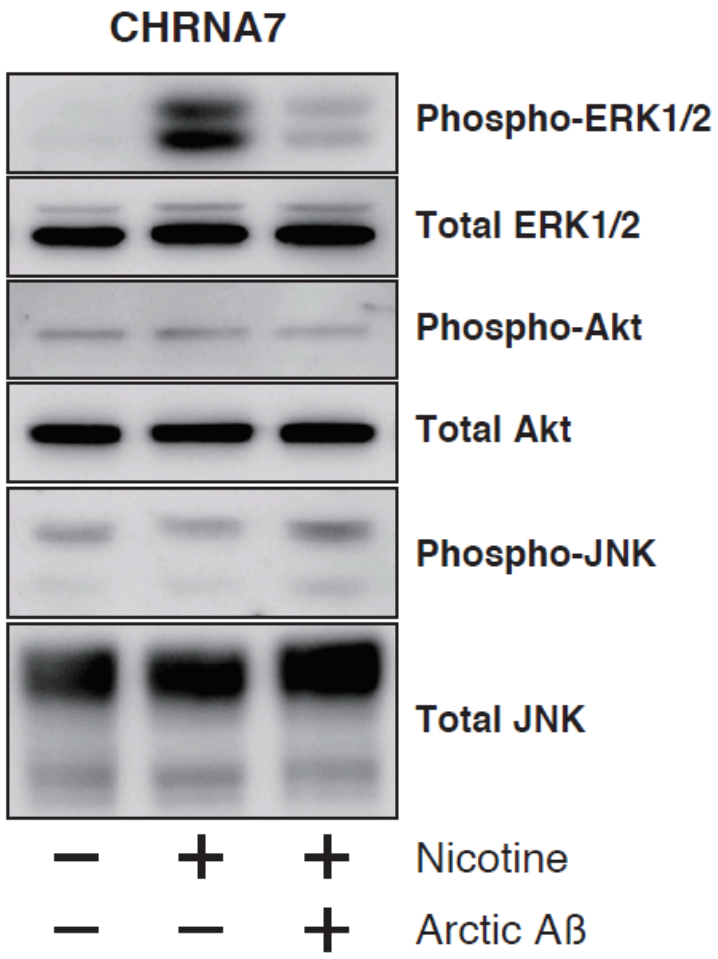

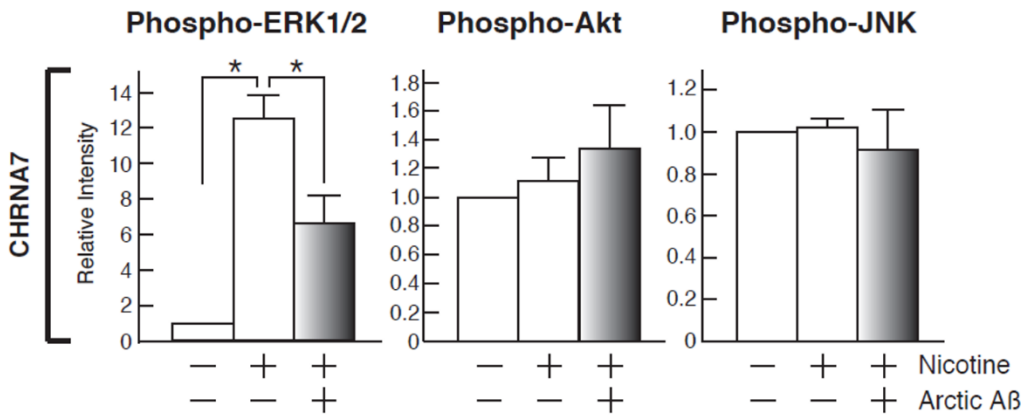

B. Mock-transfected SH-SY5Y cells

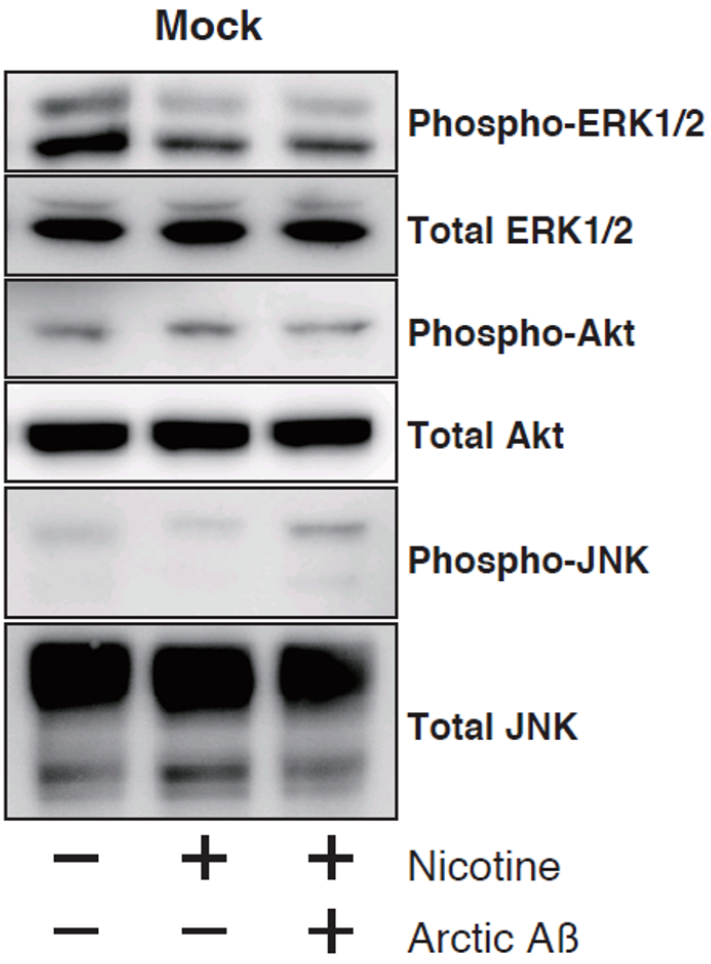

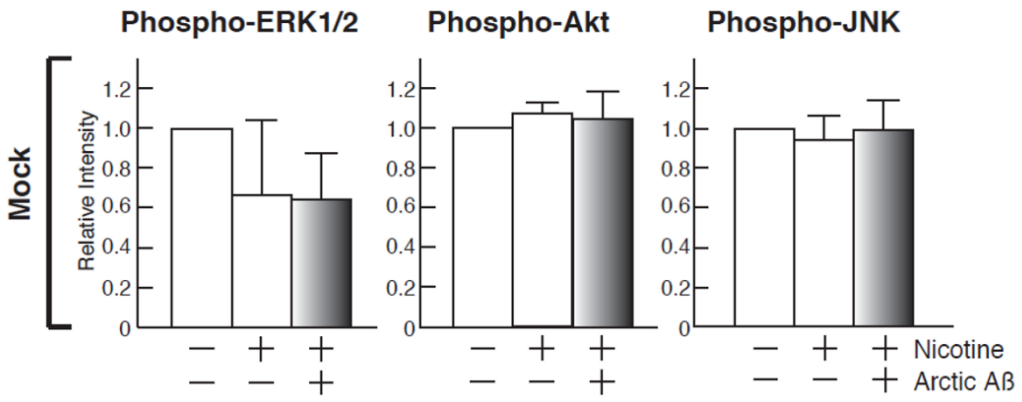

Figure 3-17 Activation of ERK1/2 was the key signaling protein participating in Arctic Aβ-mediated-interference on functions of CHRNA7 activated by nicotine

(A) From CHRNA7 over-expressed cells, addition of the Arctic Aβ only inhibits the activation of ERK1/2 but no other signaling proteins (**p<0.01). Quantification of western blot for all signaling proteins is represented as means ± SD (n=3). (B) None of the activation change of signaling proteins is observed using the SH-SY5Y cells without CHRNA7 over-expression. Quantification of western blot for all signaling proteins is represented as means ± SD (n=3).

A. PD98059 inhibited the activation of ERK1/2

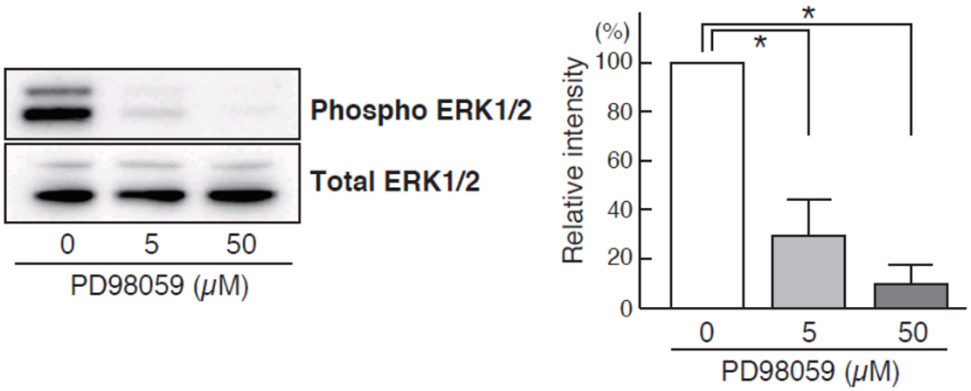

B. Neuroprotection of CHRNA7 induced by nicotine

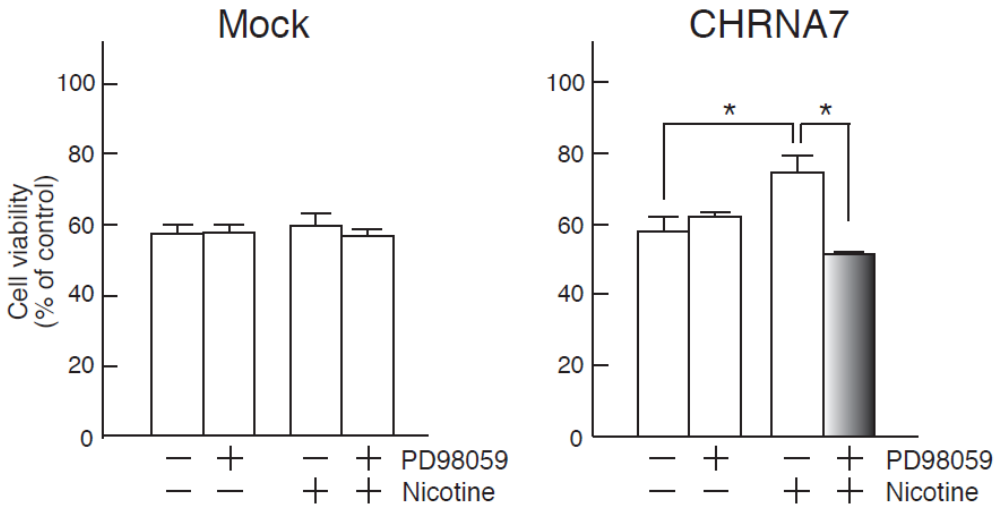

Figure 3-18 Activation of ERK1/2 mediating the nicotine effect in neuroprotection of CHRNA7 against oxidative stress induced by H_2O_2

(A) CHRNA7 was transfected into cells. 5μM and 50μM PD98059 was added for one hour prior to treating with nicotine to activate ERK1/2. 5μM and 50μM PD98059 both inhibited the activation of ERK1/2 significantly, while 50μM inhibited further (*$p<0.05$, **$p<0.01$). Quantification of western blot is represented as means ± SD (n=3). (B) From CHRNA7 over-expressed cells, addition of 5μM PD98059 significantly blocked the neuroprotective function of CHRNA7 against oxidative stress activated by nicotine (*$p<0.05$). The mock-transfected SH-SY5Y cells failed to show the nicotine-induced neuroprotection, excluding the influence of endogenous CHRNA7 in SH-SY5Y cells. Quantification of the MTS assay is represented as means ± SD (n=3).

3-9 Supplementary experiments

3-9-1 Aβ42 dose-dependently bound to CHRNA7 - N terminal with high affinity

The direct interaction of CHRNA7 with wild-type Aβ42 has already been confirmed (Figure 3-2) and Arctic Aβ was found to bind to CHRNA7 with higher affinity than wild-type (Figure 3-1, 3-2). In order to further understand interaction between CHRNA7 and Aβ, I investigated the key binding sites on CHRNA7. N-terminal extracellular membrane domain of CHRNA7 contains ligand-binding sites for Acetylcholine (ACh) and nicotine (Brejc et al. 2001; Dougherty & Stauffer 1990). Tyrosine at the position 188 in mouse CHRNA7 has been indicated primary juxtaposition and interaction of Aβ by affecting Aβ-induced CHRNA7 functions (Tong et al. 2011), which is also included in N-terminal extracellular domain of CHRNA7. Therefore, the exact key domains participating within the direct interaction between CHRNA7 and Aβ were investigated. N-terminal extracellular domain of CHRNA7 (Figure 3-19) was considered to serve the potential role within interaction of CHRNA7 with Aβ.

Firstly, GST-CHRNA7-N terminal fusion protein was produced, which contained only the N-terminal sequence of CHRNA7. The expression of this protein was confirmed using anti-CHRNA7 antibody and size was compared

with full-length CHRNA7 (Figure 3-20A). Next, I searched whether synthetic Aβ42 could bind to CHRNA-N terminal using *in vitro* binding assay, and GST-only was used as control. As the result, wild-type Aβ42 bound to CHRNA7-N terminal without the influence of GST (Figure 3-20B). Furthermore, the direct interaction of CHRNA7 with wild-type Aβ42 was dose-dependent based on the quantification of dot-blot result (Figure 3-20C).

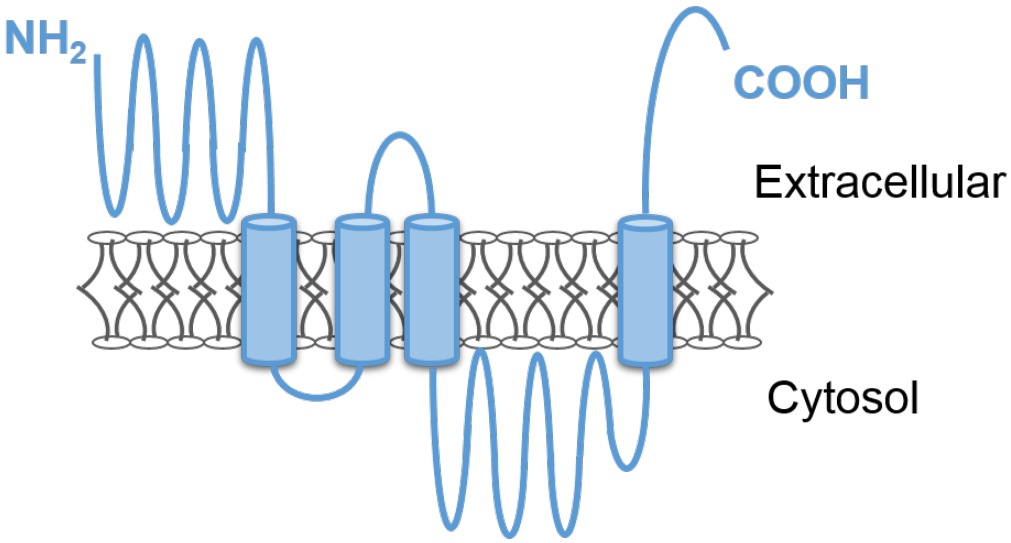

Figure 3-19 The structure of CHRNA7

CHRNA7 receptors are thought to be pentamers to be functional composed of homologous subunits. The proposed structure for each subunit is a conserved N-terminal extracellular domain followed by three conserved transmembrane domains, a variable cytoplasmic loop, a fourth conserved transmembrane domain, and a short C-terminal extracellular region. Among them, N-terminal extracellular membrane domain of CHRNA7 contains ligand-binding sites for Acetylcholine (ACh) and nicotine (Brejc et al. 2001; Dougherty & Stauffer 1990).

A. Generation of GST-CHRNA7-N-terminal protein

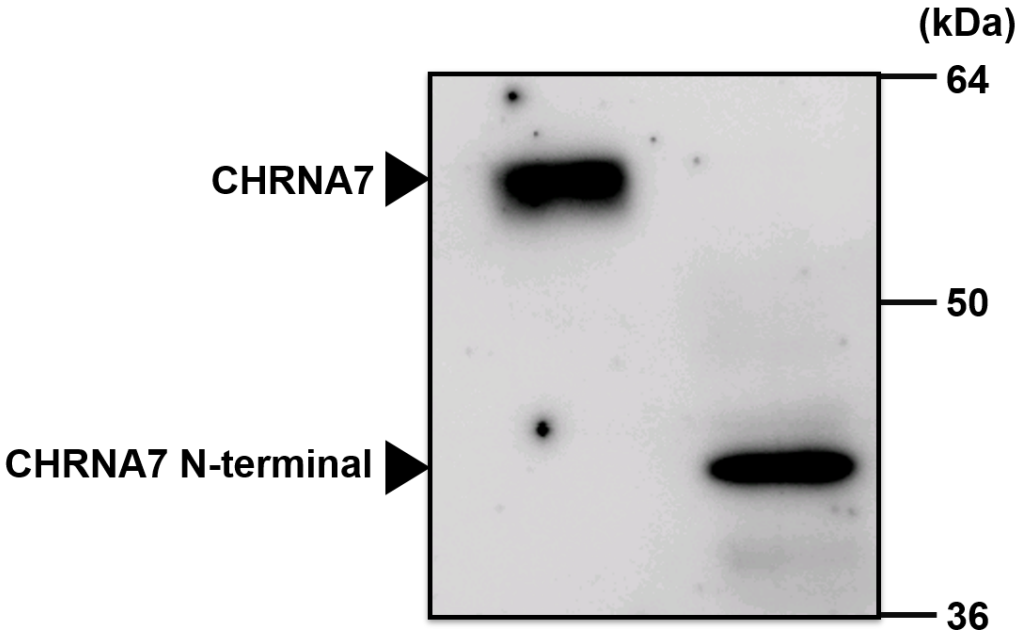

B. *in vitro* binding of GST-CHRNA7 N-terminal with Aβ42

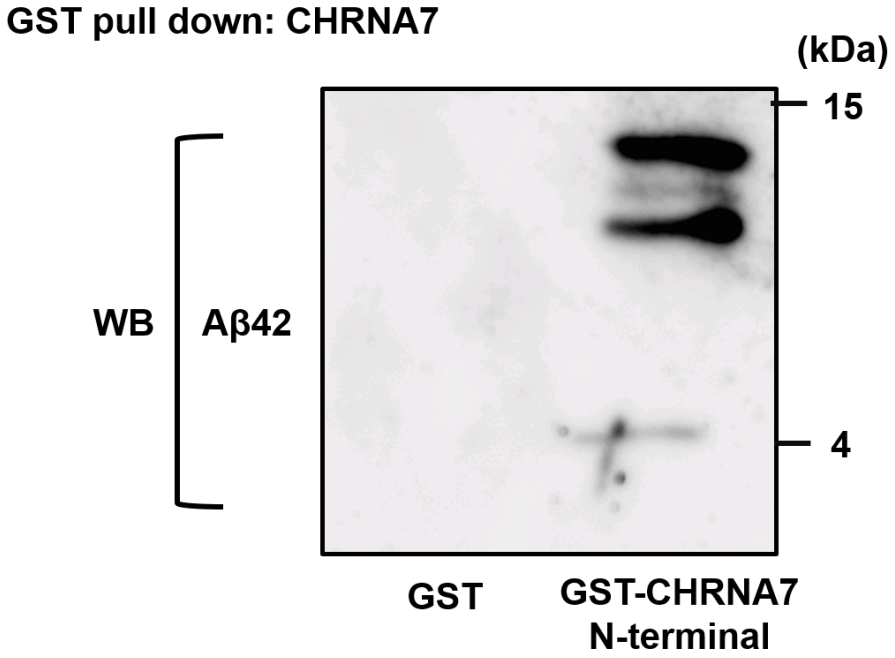

C. Aβ42 dose-dependently bound to CHRNA7-N terminal

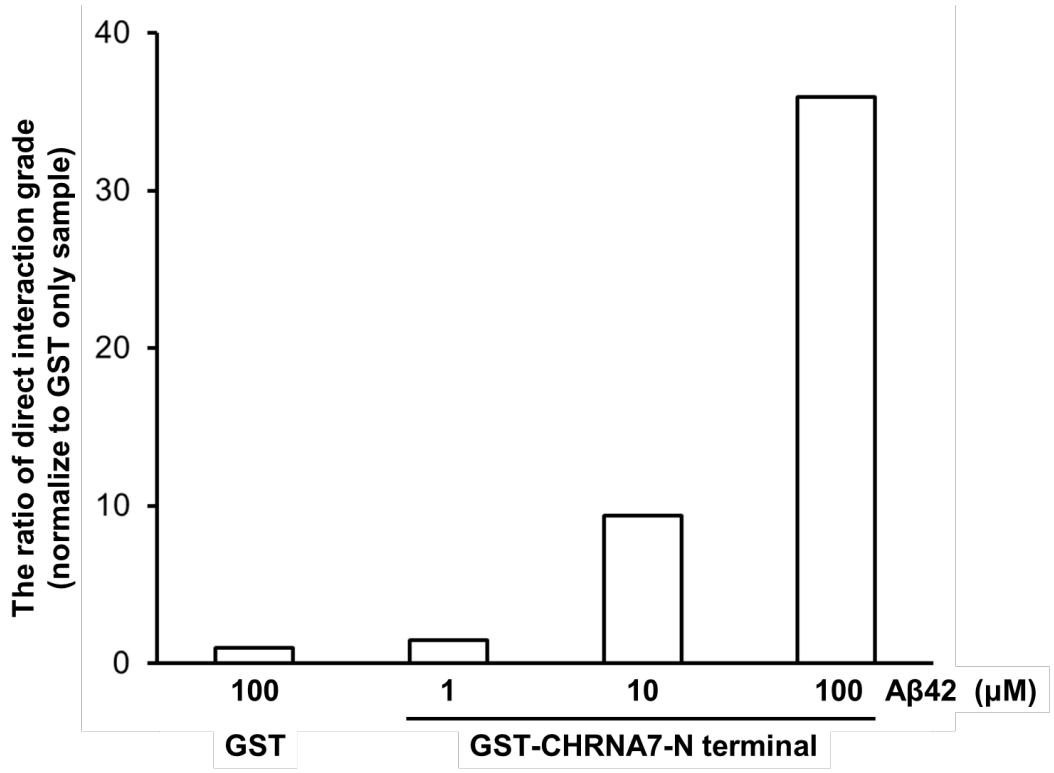

Figure 3-20 Aβ42 bound to CHRNA7 extracellular N terminal domain dose-dependently

(A) GST-CHRNA7-N terminal fusion protein was generated, which contained only the N-terminal sequence of CHRNA7. Anti-CHRNA7 antibody was used to confirm the generation of CHRNA7-N terminal protein. Size of N-terminal was compared with full-length CHRNA7. (B) Synthetic Aβ42 bound to CHRNA7-N terminal. GST-only was used as control. GST showed lack of the influence on this Aβ42 – CHRNA7-N-terminal bond. (C)

The direct interaction of CHRNA7 with wild type Aβ42 was dose-dependent based on the quantification of dot-blot result.

3-9-2 Arctic Aβ42 bound to CHRNA7 - N terminal with higher affinity than wild-type

Arctic Aβ42 was utilized to investigate the direct interaction as well. The result showed that Arctic Aβ42 bound to CHRNA7-N- terminal with higher affinity than wild-type (Figure 3-21). However, the binding of Aβ40 peptide (both Arctic mutant type and wild-type) with CHRNA-N-terminal was too weak to be detectable (data not shown).

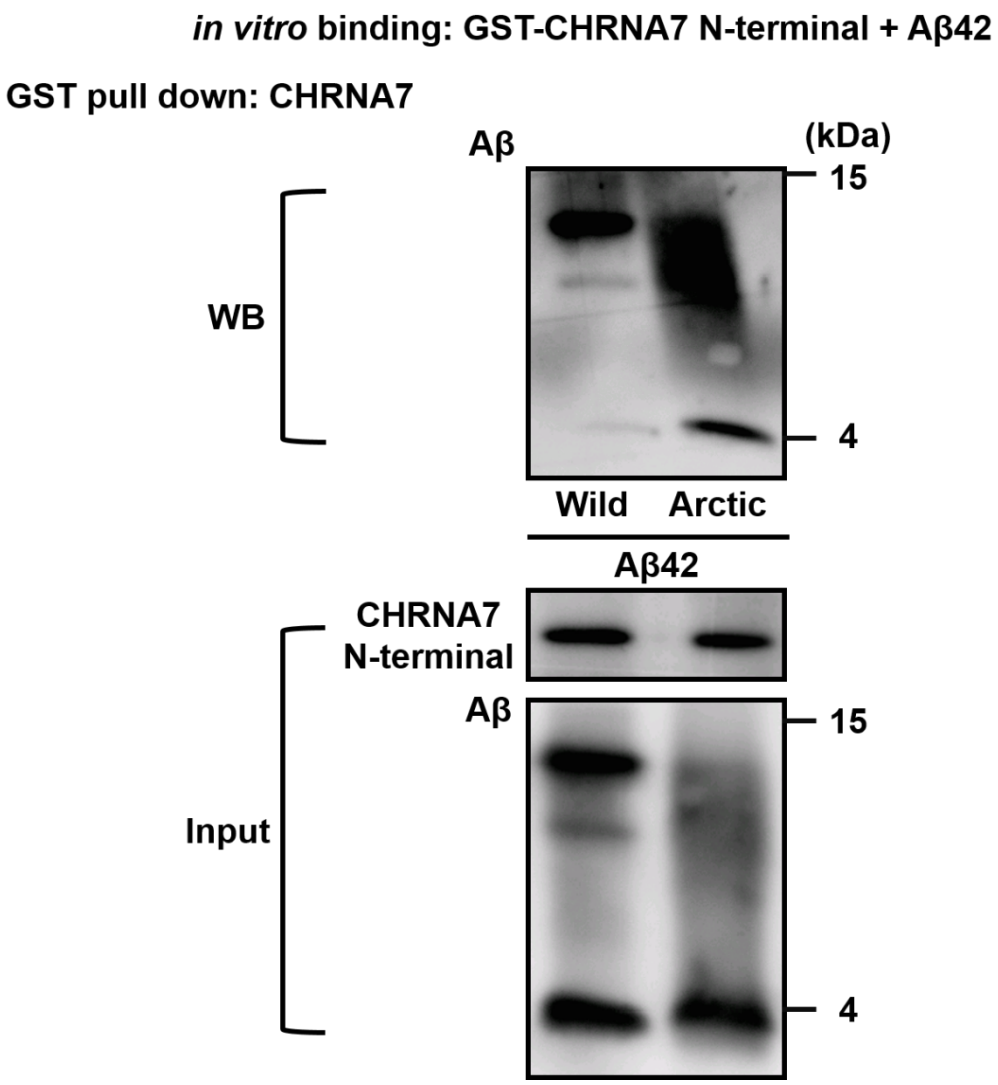

Figure 3-21 Arctic Aβ42 bound to CHRNA7-N terminal with higher affinity than wild-type

An *in vitro* binding experiment using Arctic Aβ42 and wild type Aβ42 was performed. Arctic Aβ42 binds to GST-CHRNA7-N terminal more strongly than wild type Aβ42. Bands corresponded to Aβ42 aggregated forms are also detectable. Aggregates are visible in input sample used for *in vitro*

binding experiment as well, which suggests the self-accumulation of Arctic Aβ42 and wild-type Aβ42.

3-9-3 Arctic Aβ enhanced its aggregation when co-incubated with CHRNA7 N-terminal

Arctic Aβ enhanced its aggregation when co-incubated with CHRNA7 (Figure 3-3, 3-4). Therefore, whether Arctic Aβ could appear to have the similar aggregation trend when co-incubation with CHRNA7 N-terminal using ThT assay was tested. In order to exclude the influence of accelerated accumulation ability of Aβ42 peptide, Aβ40 was utilized to do the research. Even though CHRNA7 N-terminal - Aβ40 direct bind was too weak to be detectable in previous experiment, Arctic Aβ40 aggregated further when co-incubated with CHRNA7 N-terminal (Figure 3-22). When co-incubation with CHRNA7, Arctic Aβ40 started to aggregate at 6-hr incubation time point, maximize its aggregation level at 9-hr incubation time point, and stayed its maximum aggregation to 24-hr incubation time point (Figure 3-22B). This pheromone was not observed within wild-type Aβ40 (Figure 3-22A). Among them, GST appeared to have no effect on the aggregation (Figure 3-22, blue line).

A. ThT assay of Aβ40 with or without CHNRA7 N-terminal

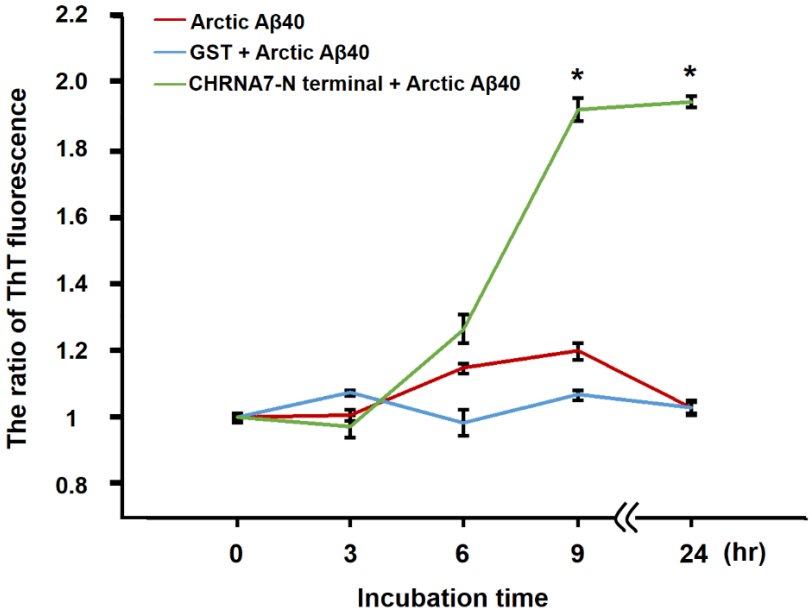

B. ThT assay of Arctic Aβ40 with or without CHNRA7 N-terminal

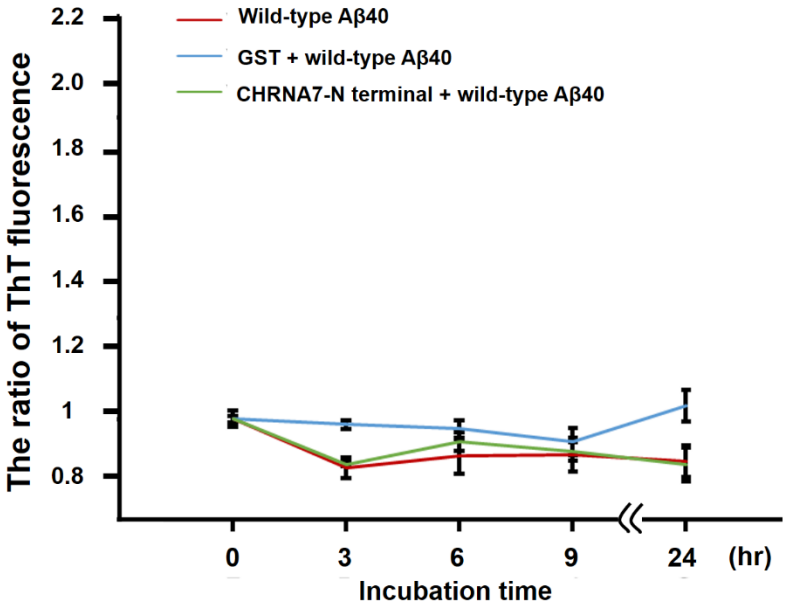

Figure 3-22 Arctic Aβ enhanced its aggregation with addition of CHRNA7 extracellular N terminal domain

The ThT assay was used to determine the aggregation form in presence of CHRNA7 extracellular N terminal domain over time. (A) Wild-type Aβ40 does not aggregate when co-incubated with CHRNA7 N-terminal nor GST protein; (B) Compare with Arctic Aβ alone, the addition of CHRNA7 N-terminal helps Arctic Aβ aggregates further (*$p<0.05$ at the time point of 9h, 24h). GST protein showed lack of the influence on the aggregation of Aβ. The data of each time point is represented as means ± SD (n=3).

3-9-4 Interference of signaling protein ERK1/2 by Aβ was specific to Arctic mutation

ERK1/2 was the key signaling protein participating in Arctic Aβ-mediated-interference on functions of CHRNA7 activated by nicotine in neuronal cells (3-8, Figure 3-17). Moreover, the activation of ERK1/2 mediated the nicotine effect in neuroprotection (3-8, Figure 3-18). In order to find out whether this effect is specific to Arctic mutation (E22G), other familial AD Aβ as well as wild-type Aβ were tested to see whether they could influence on the activation of ERK1/2 or other signaling proteins. As the result (Figure 3-23), ERK1/2 was further confirmed to be the only key signaling protein participating in Arctic Aβ-mediated-interference on functions of CHRNA7 activated by nicotine in neuronal cells. Meanwhile, this interference was found out to be specific to Arctic mutation. Nicotine was able to activated the activation of ERK1/2 in cells over-expressed with CHRNA7. The incubation of Arctic Aβ inhibited the activation of ERK1/2, while wild-type, Dutch or Iowa Aβ did not. Therefore, the inhibition of ERK1/2 participating in Aβ-mediated-interference on functions of CHRNA7 activated by nicotine in neuronal cells was found to be specific to Arctic mutation.

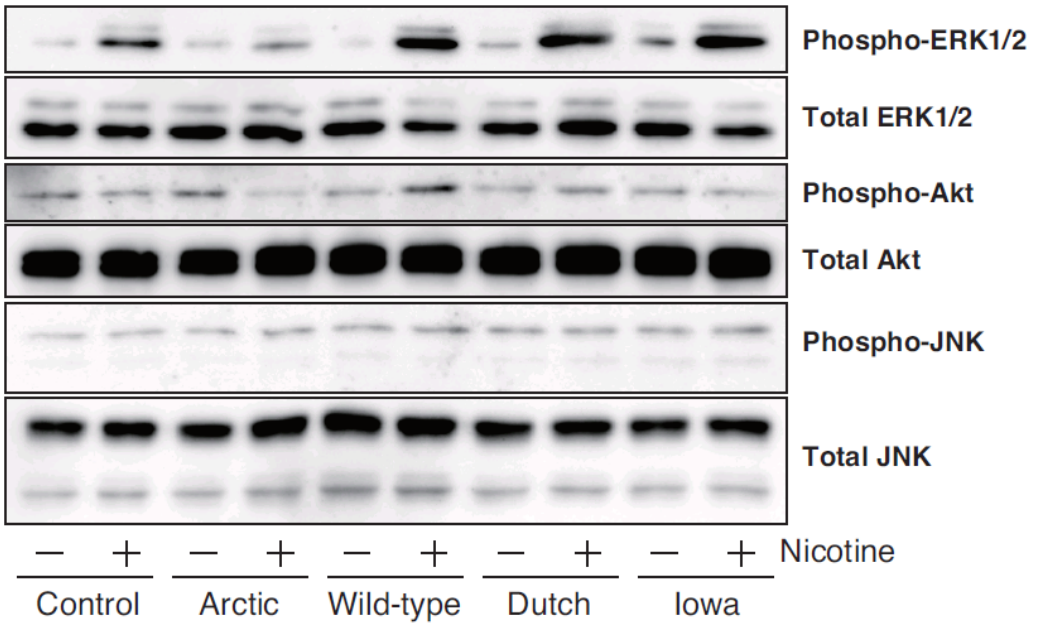

Figure 3-23 ERK1/2 participating in Aβ-mediated-interference on functions of CHRNA7 activated by nicotine was specific to Arctic mutation

CHRNA7 was transfected into the SH-SY5Y cells. Nicotine was able to activate the activation of ERK1/2. The incubation of Arctic Aβ only inhibited the activation of ERK1/2, while wild-type, Dutch or Iowa Aβ did not. As the result, ERK1/2 was the only key signaling protein participating in Arctic Aβ-mediated-interference on functions of CHRNA7 activated by nicotine in neuronal cells, and this interference was specific to Arctic mutation.

Chapter 4 Summary and Discussion

This study has shown for the first time that Arctic Aβ specifically bound to CHRNA7 with high affinity, unlike other typical early-onset FAD mutant forms of Aβ. Arctic Aβ enhanced its aggregation when co-incubated with CHRNA7, thus suggesting that this membrane receptor was required for further aggregation of this mutant form of Aβ. Furthermore, when CHO-K1 cells over-expressed CHRNA7, Arctic Aβ aggregated on CHRNA7 and inhibited the function by reducing the Ca^{2+} response and nicotine-induced activation of ERK1/2. This results clarified that CHRNA7 might be the target membrane receptor for Arctic Aβ (Ju et al. 2014). Moreover, I demonstrated that Arctic Aβ influenced the neuroprotective effect of activated CHRNA7 using SH-SY5Y cells. This interference was participated by the activation of ERK1/2 but not the other cell survival-related signaling proteins. The results gained in this study are summarized in Figure 4-1.

Arctic mutation-mediated FAD has been studied since the discovery by Nilsberth et al. (Nilsberth et al. 2001). Most of the studies have focused on the special aggregation pattern of Arctic Aβ, which prefers to form protofibril assemblies than fibrils. Similar to the conclusion made by Nilsberth et al., (Nilsberth et al. 2001), some of these studies have suggested that Arctic Aβ protofibrils are generated faster than wild type Aβ (Päiviö et al. 2004; Johansson et al. 2006). Those studies were performed under different

conditions (Johansson et al. 2006) or by structural analysis (Norlin et al. 2012). Meanwhile, there were other aspects of aggregation patterns of Arctic Aβ being studied as well. Oligomerization pattern of Arctic mutation was reported different from wild type Aβ with a tendency to form larger oligomers (Gessel et al. 2012). Fibril structures were also observed and studied previously (Norlin et al. 2012). However, none of these studies targeted any molecular signaling pathway including membrane receptors. CHRNA7 bind to wild-type Aβ42 (H. Wang et al. 2000; H.-Y. Wang et al. 2000) without any interaction with wild-type Aβ40. The result from this study (Chapter 3; 3-1; Figure 3-1) showed that Arctic Aβ40 bound to CHRNA7 with high affinity, suggesting that CHRNA7 plays a critical role in FAD caused by Arctic mutation through the interaction with Arctic Aβ. This finding suggests that the structures of monomer Arctic Aβ40 may have changed to appear the higher affinity against CHRNA7 because of its mutant effect.

N-terminal extracellular membrane domain of CHRNA7 contains ligand-binding sites for Acetylcholine (ACh) and nicotine (Brejc et al. 2001; Dougherty & Stauffer 1990). The results showed that wild-type Aβ42 bound to extracellular N terminal of CHRNA7 dose-dependently (Chapter3; 3-9-1; Figure 3-20). Furthermore, extracellular N terminal domain of CHRNA7 was determined to be the key sequence within Arctic Aβ-CHRNA7 direct interaction (Chapter 3; 3-9-1; Figure 3-21), that Arctic Aβ bound to

CHRNA7-N-terminal with higher affinity than wild-type. These results assist the explanation that extracellular N-terminal domain of CHRNA7 plays the critical role in Aβ-CHRNA7 interaction.

The aggregation pattern of Arctic Aβ40 is different from wild-type (Gessel et al. 2012) because Arctic Aβ40 can generate protofibrils faster and into a bigger size when incubated (Norlin et al. 2012; Päiviö et al. 2004). Under the experimental condition from this study, self-aggregation of Arctic Aβ40 was not seen (Chapter 3; 3-3; Figure 3-3, 3-4). Arctic Aβ40 enhanced its aggregation when co-incubated with CHRNA7 (Chapter 3; 3-3; Figure 3-3, 3-4). The co-incubation of CHRNA7-N-terminal also enhanced Arctic Aβ aggregation (Chapter 3; 3-9-2; Figure 3-22), suggesting CHRNA7-N-terminal is the key domain affecting the aggregation of Arctic Aβ. Several *in vitro* studies have reported that conditional change would affect aggregation easily: the presence of lipid enhances the Arctic Aβ aggregation (Pifer et al. 2011; Sureshbabu et al. 2010); membrane-mimicking environment is crucial for Arctic Aβ aggregation (Yamamoto et al. 2004); Mixing Arctic Aβ with wild type also enhances Arctic aggregation (Lashuel et al. 2003). There are several studies demonstrating that CHRNA7 interacts with Aβ (Wang et al. 2009), and exacerbates the pathological features in AD mouse models (Søderman et al. 2008; Dziewczapolski et al. 2009). Therefore, this study suggests that CHRNA7 may serve as the scaffold protein (seed) to enhance

the aggregation of Arctic Aβ, that N-terminal of CHRNA7 serves a critical role.

Although the direct addition of Arctic Aβ40 did not affect the Ca^{2+} flux (Chapter 3; 3-4; Figure 3-7), a diminished Ca^{2+} response was observed after a 24-h incubation of Arctic Aβ (Chapter 3; 3-5; Figure 3-10). Based on these results, the inhibition of CHRNA7 function could be the result of the aggregation of Arctic Aβ40 when both co-incubated for 24 hours. Previous study reports that Arctic Aβ40 is able to inhibit the hippocampal LTP *in vivo* (Klyubin et al. 2004). In their study, intracerebroventricular injection of Arctic Aβ40 blocked the LTP in CA1 area of the hippocampal hemisphere (Klyubin et al. 2004). Moreover, the activation of CHRNA7 at glutamatergic synapses promotes LTP (Mansvelder & McGehee 2000). Therefore, the function of CHRNA7 may be a critical intermediate, and its loss of function may be the primary cause of LTP inhibition by Arctic Aβ.

Numerous studies have revealed that CHRNA7 played as a neuroprotective role against several cell insults including different excitotoxicities in cortical (Stevens et al. 2003; Huang et al. 2012; Hejmadi et al. 2003), hippocampal neurons (J. Egea et al. 2007; Dajas-Bailador et al. 2000; Ren et al. 2007; Shin et al. 2007), as well as culture cells (Jonnala & Buccafusco 2001; Li et al. 1999; Barrio et al. 2011; Ren et al. 2005; Roensch et al. 2007). Those studies indicates that activated CHRNA7

appeared to have neuroprotective function against oxidative stress (Guan et al. 2001; Qi et al. 2013; Javier Egea et al. 2007), glutamate toxicity (Shimohama et al. 1996; Shimohama 2009; Kihara et al. 2001; Iwamoto et al. 2013; Cui et al. 2013) or other kinds of insults (Shaw et al. 2002; Dajas-Bailador et al. 2000; Shin et al. 2007; Yu et al. 2011).

The pathology of AD is associated with increased oxidative stress (Ma et al. 2011; Hensley et al. 1994; Abramov & Duchen 2005; Kamynina et al. 2013) on a molecular level. Arctic mutation-mediated FAD has also been reported the same result (Ronnback et al. 2016). Therefore, oxidative stress appeared to play an important role in the pathogenesis of AD (Qi et al. 2013; Massaad 2011). In order to search the neuroprotective function of CHRNA7, H_2O_2 was applied as an oxidative stress inducer (Wang et al. 2003) and nicotine as to activate CHRNA7 (Dajas-Bailador et al. 2000; Iwamoto et al. 2013; Shin et al. 2007) in the experiments in this study.

Neuronal cell model SH-SY5Y cells in which over-expressed with CHRNA7 can be inhibited by RNAi (Qi et al. 2007). Both of cells with the knock-down of the expression of CHRNA7 failed to represent the neuroprotective function of CHNRA7 (Chapter 3; 3-6; Figure 3-13). Arctic mutant Aβ was found to inhibit the neuroprotective function of CHRNA7 (Chapter 3; 3-7; Figure 3-15A, Figure 3-16). This phenomenon was not seen within the mock-transfected cells, indicating that this interference effect of

Arctic Aβ on the neuroprotective function was actually mediated through CHRNA7 but no other channels in SH-SY5Y cells (Figure 3-15B). Combine together, these results serve a brief interpretation that the interference of Arctic Aβ on CHRNA7 may be one of the key molecular mechanisms within the Arctic mutation-mediated FAD.

The signaling pathways that implicated in CHRNA7-mediated neuroprotection are including ERK1/2 activation in several different models, both *in vitro* such as culture cells (Dajas-Bailador et al. 2002; Ren et al. 2005; Utsugisawa et al. 2002a), and *in vivo* like neuronal cultures (Toborek et al. 2007; Dajas-Bailador et al. 2002; Dineley et al. 2001) and mouse models (Liu et al. 2007). On the contrary, some studies present that phosphorylation of ERK1/2 by nicotine is not mediated through CHRNA7 (Nakayama et al. 2001; Barrio et al. 2011; Steiner et al. 2007). The activation of Akt has also been suggested involved in the regulation of cell-survival routes (Fan et al. 2016; Shimohama 2009; Utsugisawa et al. 2002b; Kihara et al. 2001; Cui et al. 2013; Barrio et al. 2011; Huang et al. 2012). Some results also reveal that JNK phosphorylation co-relate with the down-regulation of Akt (Huang et al. 2012) enhancement at the neuroprotection function, while some indicate that JNK do not participate in such mechanism (Ren et al. 2005; Toborek et al. 2007; Liu et al. 2007; Buckinham et al. 2009). Some studies report that CHRNA7-mediated neuroprotection involves the

inhibition of JNK without modifying ERK (Suzuki et al. 2006). Combine together, the signaling proteins participating in cell-survival routes remain controversy. Above all, the signaling proteins involved in the nicotine-mediated functions of CHRNA7 on which Arctic mutant Aβ affects are remained to be searched. The results illustrated that only ERK1/2 activation but not Akt or JNK was participating in the nicotine-mediated functions through CHRNA7, that incubated Arctic Aβ only inhibited ERK activation (Chapter 3; 3-8; Figure 3-17). Although similar result was gained when I searched the Ca^{2+} down-stream signal, signaling pathways differ within distinct cell types (Roberts et al. 2002) thus worth searching. Furthermore, activation of ERK1/2 was also confirmed to be mediating the nicotine effect in neuroprotection against oxidative stress induced by H_2O_2, by gaining the result that selective inhibitor PD98059 of ERK1/2 blocked the neuroprotection of CHRNA7 activated by nicotine (Chapter 3; 3-8; Figure 3-18). This inhibition of ERK1/2 participating in Aβ-mediated-interference on functions of CHRNA7 activated by nicotine in neuronal cells was found to be specific to Arctic mutation, but no other familial AD Aβ (Chapter 3; 3-9; Figure 3-23).

The observation of cognitive deficits in an Arctic APP transgenic mouse model (Ronnback et al. 2012; Ronnback et al. 2011) suggests that memory and cognitive functions are affected by the Arctic mutation. The levels of Aβ

protofibrils correlate with learning performance in Arctic APP mice (Lord et al. 2009), thus suggesting a link between aggregation and memory. Even though wild-type Aβ42 has been reported to activate the function of CHRNA7 (Dineley et al. 2002; Tong et al. 2011), Arctic Aβ40 inhibited the functions as well as neuroprotective effect of CHRNA7 in this study. I consider that mutation of Aβ might change its influence on CHRNA7. Loss of function of CHRNA7 enhances Aβ oligomer accumulation, exacerbating early-stage cognitive decline and septohippocampal pathology in a mouse model of AD (Hernandez et al. 2010). This previous study suggests that loss of CHRNA7 could accelerate the AD symptoms (Hernandez et al. 2010). On the contrary, deletion of CHRNA7 gene improves cognitive deficits and synaptic pathology in a mouse model of AD (Dziewczapolski et al. 2009). These reports indicate that the exact roles of CHRNA7 participating in AD pathology remains controversial. However, mice samples utilized in these groups are in different ages: 5-month mice were used for behavioral test in Hernandez's group (Hernandez et al. 2010) and around 15-month mice were used in Dziewczapolski's group (Dziewczapolski et al. 2009). Distinct ages of mice influence the accumulation of Aβ, that soluble non-fibrillar structures are generated in young mice while fibrillar-like structures are formed in elder ones. Since soluble non-fibrillar Aβ forms would affect synapse dysfunction through calcium impairment, long term potentiation

(LTP) blockage and synapse loss (Shankar & Walsh 2009; Tu et al. 2014; Palop & Mucke 2010)，and CHRNA7 is mainly located in synapse yields regulating Ca^{2+}, Ca^{2+}-dependent events and LTP (Bertrand et al. 1993; Liu et al. 2001; Mansvelder & McGehee 2000; Séguéla et al. 1993), a possible explanation for the comparative results of the exact roles of CHRNA7 participating in AD pathology is due to distinct aggregation forms of Aβ in distinct ages. Furthermore, this explanation also assists the hypothesis for understanding early-onset AD (EOAD) rather than late-onset AD(LOAD). Based on the results from this study, I think that the inhibition of the function of CHRNA7 is due to a combination of mutant effect and the higher affinity to CHRNA7. This finding led us to clarify the mechanism of Arctic FAD other than its special aggregation pattern. The findings assist the novel understanding of the molecular mechanism of Arctic mutation-mediated FAD. I hypothesize that CHRNA7-mediated changes of Arctic Aβ aggregation may be crucial for CHRNA7 in FAD caused by the Arctic mutation, which interferes the function of CHRNA7 including Ca^{2+} response and the neuroprotective characteristic. This leads to a proposal that CHRNA7 can a critical therapeutic target for the treatment of FAD caused by Arctic mutation.

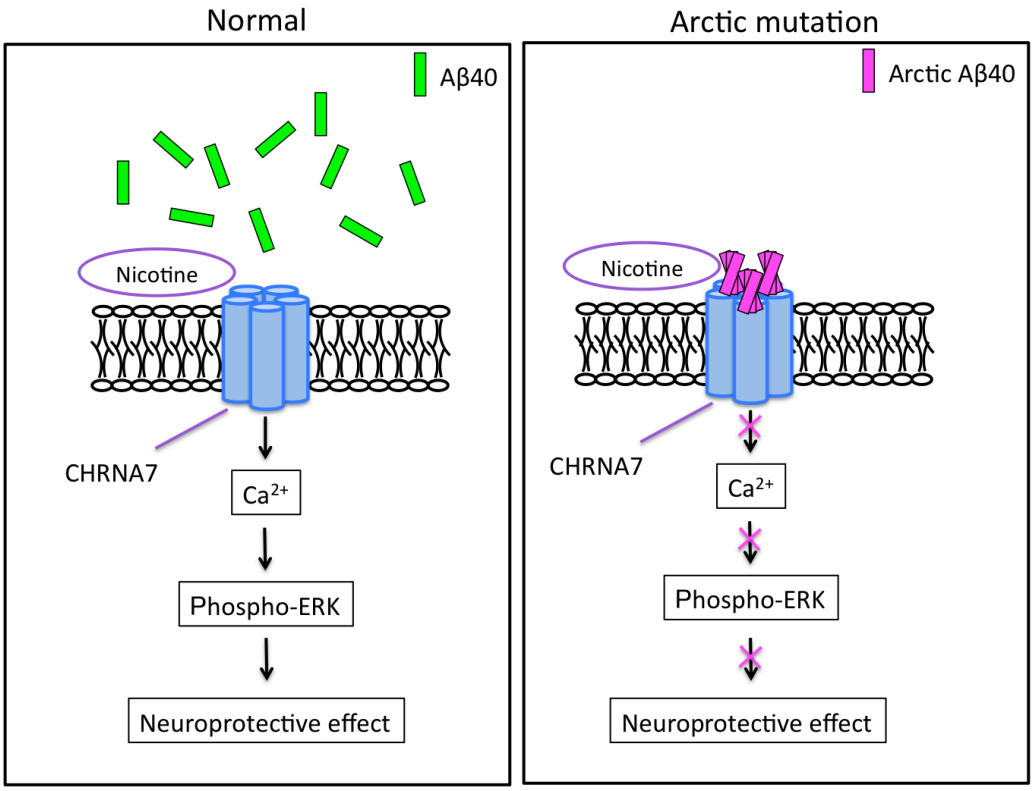

Figure 4-1 Interpreted mechanism of Arctic-mutation-mediated-FAD

Arctic Aβ specifically bound to CHRNA7 with high affinity, enhanced its aggregation and inhibited the function by reducing the Ca^{2+} response and nicotine-induced activation of ERK1/2. Moreover, Arctic Aβ influenced the neuroprotective effect of activated CHRNA7, and this interference was participated by the activation of ERK1/2 but not the other cell survival-related signaling proteins.

References

Abramov, A.Y. & Duchen, M.R., 2005. The role of an astrocytic NADPH oxidase in the neurotoxicity of amyloid beta peptides. *Phil. Trans. R. Soc. B*, 360(1464), pp.2309–2314.

Barrio, L. del et al., 2011. Neurotoxicity induced by okadaic acid in the human neuroblastoma SH-SY5Y line can be differentially prevented by α7 and β2* nicotinic stimulation. *Toxicol. Sci.*, 123(1), pp.193–205.

Basun, H. et al., 2008. Clinical and neuropathological features of the arctic APP gene mutation causing early-onset Alzheimer disease. *Arch. Neurol.*, 65(4), pp.499–505.

Bengtson, C.P. et al., 2013. Calcium responses to synaptically activated bursts of action potentials and their synapse-independent replay in cultured networks of hippocampal neurons. *Biochim. Biophys. Acta*, 1833(7), pp.1672–1679.

Bertram, L. & Tanzi, R.E., 2004. Alzheimer's disease: one disorder, too many genes? *Hum. Mol. Genet.*, 13, pp.R135–141.

Bertrand, D. et al., 1993. Mutations at two distinct sites within the channel domain M2 alter calcium permeability of neuronal α7 nicotinic receptor. *Proc. Natl. Acad. Sci. USA*, 90(15), pp.6971–6975.

Biancalana, M. & Koide, S., 2010. Molecular Mechanism of Thioflavin-T Binding to Amyloid Fibrils. *Biochim Biophys Acta.*, 1804(7), pp.1405–1412.

Brejc, K. et al., 2001. Crystal structure of an ACh-binding protein reveals the ligand-binding domain of nicotinic receptors. *Nature*, 411(6835), pp.269–276.

Van Broeckhoven, C. et al., 1990. Amyloid beta protein precursor gene and hereditary cerebral hemorrhage with amyloidosis (Dutch). *Science*, 248(4959), pp.1120–1122.

Brookmeyer, R. et al., 2007. Forecasting the global burden of Alzheimer's disease. *Alzheimer's and Dementia*, 3(3), pp.186–191.

Brusés, J.L., Chauvet, N. & Rutishauser, U., 2001. Membrane lipid rafts are necessary for the maintenance of the (alpha)7 nicotinic acetylcholine receptor in somatic spines of ciliary neurons. *J. Neurosci.*, 21(2), pp.504–512.

Buckinham, S.D. et al., 2009. Nicotinic acetylcholine receptor signalling: roles in Alzheimer's disease and amyloid neuroprotection. *Pharmacol. Rev.*, 61(1), pp.39–61.

Burdick, D. et al., 1992. Assembly and aggregation properties of synthetic

Alzheimer's A4/beta amyloid peptide analogs. *J. Biol. Chem.*, 267(1), pp.546–554.

Cavanaugh, J.E. et al., 2006. Spinal AMPA receptor inhibition attenuates mechanical allodynia and neuronal hyperexcitability following spinal cord injury in rats. *J. Neurosci. Res.*, 84, pp.1367–1375.

Di Cesare Mannelli, L. et al., 2014. Involvement of α7 nAChR subtype in rat oxaliplatin-induced neuropathy: effects of selective activation. *Neuropharmacology*, 79, pp.37–48.

Cheng, I.H. et al., 2007. Accelerating amyloid-β fibrillization reduces oligomer levels and functional deficits in Alzheimer disease mouse models. *J. Biol. Chem.*, 282(33), pp.23818–23828.

Cheung, Y.T. et al., 2009. Effects of all-trans-retinoic acid on human SH-SY5Y neuroblastoma as in vitro model in neurotoxicity research. *Neurotoxicology*, 30(1), pp.127–135.

Cui, W. et al., 2013. Bis(12)-hupyridone, a novel acetylcholinesterase inhibitor, protects against glutamate-induced neuronal excitotoxicity via activating α7 nicotinic acetylcholine receptor/phosphoinositide 3-kinase/Akt cascade. *Chem. Biol. Interact.*, 203(1), pp.365–370..

Dahlgren, K.N. et al., 2002. Oligomeric and fibrillar species of amyloid-β

peptides differentially affect neuronal viability. *J. Biol. Chem.*, 277(35), pp.32046–32053.

Dajas-Bailador, F.A., Lima, P.A. & Wonnacott, S., 2000. The alpha7 nicotinic acetylcholine receptor subtype mediates nicotine protection against NMDA excitotoxicity in primary hippocampal cultures through a Ca2+ dependent mechanism. *Neuropharmacology*, 39(13), pp.2799–2807.

Dajas-Bailador, F.A., Soliakov, L. & Wonnacott, S., 2002. Nicotine activates the extracellular signal-regulated kinase 1/2 via the alpha7 nicotinic acetylcholine receptor and protein kinase A, in SH-SY5Y cells and hippocampal neurones. *J. Neurochem.*, 80(3), pp.520–530.

Dineley, K.T. et al., 2001. β-Amyloid Activates the Mitogen-Activated Protein Kinase Cascade via Hippocampal α7 Nicotinic Acetylcholine Receptors: In Vitro and In Vivo Mechanisms Related to Alzheimer's Disease. *J. Neurosci.*, 21(12), pp.4125–4133.

Dineley, K.T. et al., 2002. β-Amyloid peptide activates α7 nicotinic acetylcholine receptors expressed in Xenopus oocytes. *J. Biol. Chem.*, 277(28), pp.25056–25061.

Dougherty, D.A. & Stauffer, D.A., 1990. Acetylcholine binding by a synthetic receptor: implications for biological recognition. *Science*,

250(4987), pp.1558–1560.

Dziewczapolski, G. et al., 2009. Deletion of the alpha 7 nicotinic acetylcholine receptor gene improves cognitive deficits and synaptic pathology in a mouse model of Alzheimer's disease. *J. Neurosci.*, 29(27), pp.8805–8815.

Egea, J. et al., 2007. Neuroprotection afforded by nicotine against oxygen and glucose deprivation in hippocampal slices is lost in alpha7 nicotinic receptor knockout mice. *Neuroscience*, 145(3), pp.866–872.

Egea, J. et al., 2007. Nicotinic receptor activation by epibatidine induces heme oxygenase-1 and protects chromaffin cells against oxidative stress. *J. Neurochem.*, 102(6), pp.1842–1852.

Ehehalt, R. et al., 2003. Amyloidogenic processing of the Alzheimer beta-amyloid precursor protein depends on lipid rafts. *J. Cell Biol.*, 160(1), pp.113–123.

Fan, Y.L. et al., 2016. Curcumin Attenuated Bupivacaine-Induced Neurotoxicity in SH-SY5Y Cells Via Activation of the Akt Signaling Pathway. *Neurochem. Res.* 41(9), pp2425-2432

Fernandez-Gomez, F.J. et al., 2006. Pyruvate protects cerebellar granular cells from 6-hydroxydopamine-induced cytotoxicity by activating the

Akt signaling pathway and increasing glutathione peroxidase expression. *Neurobiol. Dis.*, 24(2), pp.296–307.

Gessel, M.M. et al., 2012. Familial Alzheimers disease mutations differentially alter amyloid beta-protein oligomerization. *ACS Chem. Neurosci.*, 3(11), pp.909–918.

Glenner, G.G. & Wong, C.W., 1984. Alzheimer's disease: Initial report of the purification and characterization of a novel cerebrovascular amyloid protein. *Biochem. Biophys. Res. Commun.*, 120(3), pp.885–890.

Grabowski, T.J. et al., 2001. Novel amyloid precursor protein mutation in an Iowa family with dementia and severe cerebral amyloid angiopathy. *Ann. Neurol.*, 49(6), pp.697–705.

Guan, Z.-Z. et al., 2001. Reduced expression of neuronal nicotinic acetylcholine receptors during the early stages of damage by oxidative stress in PC12 cells. *J. Neurosci. Res.*, 66(4), pp.551–8.

Haass, C., 2004. Take five--BACE and the γ-secretase quartet conduct Alzheimer's amyloid β-peptide generation. *EMBO J.*, 23(3), pp.483–488.

Haass, C. & Selkoe, D.J., 2007. Soluble protein oligomers in

neurodegeneration: lessons from the Alzheimer's amyloid beta-peptide. *Nat. Rev. Mol. Cell Biol.*, 8(2), pp.101–112.

Hejmadi, M. V. et al., 2003. Neuroprotection by nicotine against hypoxia-induced apoptosis in cortical cultures involves activation of multiple nicotinic acetylcholine receptor subtypes. *Mol. Cell. Neurosci.*, 24(3), pp.779–786.

Hensley, K. et al., 1994. A model for beta-amyloid aggregation and neurotoxicity based on free radical generation by the peptide: relevance to Alzheimer disease. *Proc. Natl. Acad. Sci. USA*, 91(8), pp.3270–3274.

Hernandez, C.M. et al., 2010. Loss of α7 Nicotinic Receptors Enhances β-Amyloid Oligomer Accumulation , Exacerbating Early-Stage Cognitive Decline and Septohippocampal Pathology in a Mouse Model of Alzheimer ' s Disease. *J. Neurosci.*, 30(7), pp.2442–2453.

Hotokezaka, H. et al., 2002. U0126 and PD98059, specific inhibitors of MEK, accelerate differentiation of RAW264.7 Cells into osteoclast-like cells. *J. Biol. Chem.*, 277(49), pp.47366–47372.

Hsiao, K. et al., 1996. Correlative Memory Deficits, Abeta Elevation, and Amyloid Plaques in Transgenic Mice. *Science*, 274, pp.99–102.

Huang, X. et al., 2012. Neuroprotection by nicotine against colchicine-induced apoptosis is mediated by PI3-kinase-Akt pathways. *Int. J. Neurosci.*, 122(6), pp.324–332.

Itkin, A. et al., 2011. Calcium ions promote formation of amyloid β-peptide (1-40) oligomers causally implicated in neuronal toxicity of Alzheimer's disease. *PLoS ONE*, 6(3).

Iwamoto, K. et al., 2013. Neuroprotection of rat retinal ganglion cells mediated through alpha7 nicotinic acetylcholine receptors. *Neuroscience*, 237, pp.184–198.

Jarrett, J.T., Berger, E.P. & Lansbury, P.T., 1993. The carboxy terminus of the beta amyloid protein is critical for the seeding of amyloid formation: implications for the pathogenesis of Alzheimer's disease. *Biochemistry*, 32(18), pp.4693–4697.

Johansson, A.S. et al., 2006. Physiochemical characterization of the Alzheimer's disease-related peptides Aβ1-42Arctic and Aβ1-42wt. *FEBS J.*, 273(12), pp.2618–2630.

Jonnala, R.R. & Buccafusco, J.J., 2001. Relationship between the increased cell surface α7 nicotinic receptor expression and neuroprotection induced by several nicotinic receptor agonists. *J. Neurosci. Res.*, 66(4), pp.565–572.

Ju, Y., Asahi, T. & Sawamura, N., 2014. Arctic mutant Aβ40 aggregates on α7 nicotinic acetylcholine receptors and inhibits their functions. *J. Neurochem.*, 131(5), pp.667–674.

Kamino, K. et al., 1992. Linkage and mutational analysis of familial Alzheimer disease kindreds for the APP gene region. *Am. J. Hum. Genet.*, 51(5), pp.998–1014.

Kamynina, A. V. et al., 2013. Acetylcholine and antibodies against the acetylcholine receptor protect neurons and astrocytes against beta-amyloid toxicity. *Int. J. Biochem. Cell Biol.*, 45(4), pp.899–907.

Kihara, T. et al., 2001. Alpha7 Nicotinic Receptor Transduces Signals to PI3 kinase to Block Aβ-induced Neurotoxicity. *J. Biol. Chem.*, 276(17), pp.13541–13546.

Kirkitadze, M.D. & Kowalska, A., 2005. Molecular mechanisms initiating amyloid beta-fibril formation in Alzheimer's disease. *Acta Biochim. Pol.*, 52(2), pp.417–423.

Klyubin, I. et al., 2004. Soluble Arctic amyloid β protein inhibits hippocampal long-term potentiation in vivo. *Eur. J. Neurosci.*, 19(10), pp.2839–2846.

Lashuel, H.A. et al., 2003. Mixtures of wild-type and a pathogenic (E22G)

form of Aβ40 in vitro accumulate protofibrils, including amyloid pores. *J. Mol. Biol.*, 332(4), pp.795–808.

LeVine, H., 1993. Thioflavine T interaction with synthetic Alzheimer's disease β-amyloid peptides: Detection of amyloid aggregation in solution. *Protein Sci.*, 2(3), pp.404–410.

Levites, Y. et al., 2002. Attenuation of 6-hydroxydopamine (6-OHDA) - induced nuclear factor-kappaB (NF- kB) activation and cell death by tea extracts in neuronal cultures. *Biochem Pharmacol*, 63, pp.21–29.

Li, Y. et al., 1999. alpha7 nicotinic receptor mediated protection against ethanol-induced cytotoxicity in Pc12 cells. *Brain Res.*, 816(1), pp.225–228.

Liu, Q. et al., 2007. Dissecting the signaling pathway of nicotine-mediated neuroprotection in a mouse Alzheimer disease model. *FASEB J.*, 21(1), pp.61–73.

Liu, Q., Kawai, H. & Berg, D.K., 2001. beta-Amyloid peptide blocks the response of alpha 7-containing nicotinic receptors on hippocampal neurons. *Proc. Natl. Acad. Sci. USA*, 98(8), pp.4734–4739.

Liu, Y. et al., 2012. alpha7 nicotinic acetylcholine receptor-mediated neuroprotection against dopaminergic neuron loss in an MPTP mouse

model via inhibition of astrocyte activation. *J Neuroinflamm.*, 9(98).

Lord, A. et al., 2009. Amyloid beta protofibril levels correlate with spatial learning in Arctic Alzheimer's disease transgenic mice. *FEBS J.*, 276(4), pp.995–1006.

Ma, T. et al., 2011. Amyloid beta-induced impairments in hippocampal synaptic plasticity are rescued by decreasing mitochondrial superoxide. *J. Neurosci.*, 31(15), pp.5589–5595.

Mansvelder, H.D. & McGehee, D.S., 2000. Long-Term Potentiation of Excitatory Inputs to Brain Reward Areas by Nicotine. *Neuron*, 27(2), pp.349–357.

Martin, S.E., De Fiebre, N.E.C. & De Fiebre, C.M., 2004. The α7 nicotinic acetylcholine receptor-selective antagonist, methyllycaconitine, partially protects against β-amyloid 1-42 toxicity in primary neuron-enriched cultures. *Brain Res.*, 1022(1-2), pp.254–256.

Massaad, C.A., 2011. Neuronal and vascular oxidative stress in Alzheimer's disease. *Curr. Neuropharmacol.*, 9(4), pp.662–673.

Miller, B.L. & Boeve, B.F., 2009. *The Behavioral Neurology of Dementia*.

Murakami, K. et al., 2003. Neurotoxicity and physicochemical properties of Aβ mutant peptides from cerebral amyloid angiopathy: Implication for

the pathogenesis of cerebral amyloid angiopathy and Alzheimer's disease. *J. Biol. Chem.*, 278(46), pp.46179–46187.

Nakayama, H. et al., 2001. Nicotine-induced phosphorylation of extracellular signal-regulated protein kinase and CREB in PC12h cells. *J. Neurochem.*, 79(3), pp.489–498.

Nilsberth, C. et al., 2001. The "Arctic" APP mutation (E693G) causes Alzheimer's disease by enhanced Abeta protofibril formation. *Nat. Neurosci.*, 4(9), pp.887–893.

Norlin, N. et al., 2012. Aggregation and fibril morphology of the Arctic mutation of Alzheimer's Abeta peptide by CD, TEM, STEM and in situ AFM. *J. Struct. Biol.*, 180(1), pp.174–189.

Ono, K. et al., 2008. Effects of grape seed-derived polyphenols on amyloid β-protein self-assembly and cytotoxicity. *J. Biol. Chem.*, 283(47), pp.32176–32187.

Päiviö, A. et al., 2004. Unique physicochemical profile of β-amyloid peptide variant Aβ1-40E22G protofibrils: Conceivable neuropathogen in arctic mutant carriers. *J. Mol. Biol.*, 339(1), pp.145–159.

Palop, J.J. & Mucke, L., 2010. Amyloid-beta-induced neuronal dysfunction in Alzheimer's disease: from synapses toward neural networks. *Nat.*

Neurosci., 13(7), pp.812–818.

Pettit, D.L., Shao, Z. & Yakel, J.L., 2001. β-Amyloid(1-42) peptide directly modulates nicotinic receptors in the rat hippocampal slice. *J. Neurosci.*, 21(1), p.RC120.

Pifer, P.M., Yates, E.A. & Legleiter, J., 2011. Point mutations in Abeta result in the formation of distinct polymorphic aggregates in the presence of lipid bilayers. *PLoS ONE*, 6(1).

Qi, X.L. et al., 2013. Preventing expression of the nicotinic receptor subunit α7 in SH-SY5Y cells with interference RNA indicates that this receptor may protect against the neurotoxicity of Aβ. *Neurochem. Res.*, 38(5), pp.943–950.

Qi, X.L. et al., 2007. The consequences of reducing expression of the alpha7 nicotinic receptor by RNA interference and of stimulating its activity with an a7 agonist in SH-SY5Y cells indicate that this receptor plays a neuroprotective role in connection with the pathogenesis o. *Neurochem. Int.*, 51(6-7), pp.377–383.

Ren, K. et al., 2005. Multiple calcium channels and kinases mediate α7 nicotinic receptor neuroprotection in PC12 cells. *J. Neurochem.*, 94(4), pp.926–933.

Ren, K. et al., 2007. α7 Nicotinic receptor gene delivery into mouse hippocampal neurons leads to functional receptor expression, improved spatial memory-related performance, and tau hyperphosphorylation. *Neuroscience*, 145(1), pp.314–322.

Roberson, E.D. & Mucke, L., 2006. 100 Years and Counting: Prospecs for Defeating Alzheimer's Disease. *Science*, 314(5800), pp.781–784.

Roberts, E.C. et al., 2002. Distinct Cell Cycle Timing Requirements for Extracellular Signal-Regulated Kinase and Phosphoinositide 3-Kinase Signaling Pathways in Somatic Cell Mitosis Distinct Cell Cycle Timing Requirements for Extracellular Signal-Regulated Kinase and Phosphoinositi. *Mol. Cell. Biol.*, 22(20), pp.7226–7241.

Roensch, J. et al., 2007. Effects of statins on alpha7 nicotinic receptor, cholinesterase and alpha-form of secreted amyloid precursor peptide in SH-SY5Y cells. *Neurochem. Int.*, 50(6), pp.800–806.

Ronnback, A. et al., 2012. Amyloid neuropathology in the single Arctic APP transgenic model affects interconnected brain regions. *Neurobio. Aging*, 33(4), pp.831.e11–831.e19.

Ronnback, A. et al., 2016. Mitochondrial dysfunction in a transgenic mouse model expressing human amyloid precursor protein (APP) with the Arctic mutation. *J. Neurochem.*, 136(3), pp.497–502.

Ronnback, A. et al., 2011. Progressive neuropathology and cognitive decline in a single Arctic APP transgenic mouse model. *Neurobio. Aging*, 32(2), pp.280–292.

Sakono, M. & Zako, T., 2010. Amyloid oligomers: Formation and toxicity of Abeta oligomers. *FEBS Journal*, 277(6), pp.1348–1358.

Sandberg, A. et al., 2010. Stabilization of neurotoxic Alzheimer amyloid-beta oligomers by protein engineering. *Proc. Natl. Acad. Sci. USA*, 107(35), pp.15595–15600.

Sawamura, N. et al., 2005. A form of DISC1 enriched in nucleus: altered subcellular distribution in orbitofrontal cortex in psychosis and substance/alcohol abuse. *Proc. Natl. Acad. Sci. USA*, 102(4), pp.1187–1192.

Sawamura, N. et al., 2001. Site-specific phosphorylation of tau accompanied by activation of mitogen-activated protein kinase (MAPK) in brains of Niemann-Pick type C mice. *J. Biol. Chem.*, 276(13), pp.10314–10319.

Séguéla, P. et al., 1993. Molecular cloning, functional properties, and distribution of rat brain alpha 7: a nicotinic cation channel highly permeable to calcium. *J. Neurosci.*, 13(2), pp.596–604.

Selkoe, D.J., 1998. The cell biology of beta-amyloid precursor protein and presenilin in Alzheimer's disease. *Trends Cell Biol.*, 8(11), pp.447–453.

Selkoe, D.J., 1999. Translating cell biology into therapeutic advances in Alzheimer's disease. *Nature*, 399(6738), pp.A23–A31.

Shankar, G.M. & Walsh, D.M., 2009. Alzheimer's disease: synaptic dysfunction and Abeta. *Mol. Neurodegener.*, 4(1), p.48.

Shaw, S., Bencherif, M. & Marrero, M.B., 2002. Janus kinase 2, an early target of alpha7 nicotinic acetylcholine receptor-mediated neuroprotection against Abeta-(1-42) amyloid. *J. Biol. Chem.*, 277(47), pp.44920–44924.

Shimohama, S., 2009. Nicotinic receptor-mediated neuroprotection in neurodegenerative disease models. *Biol. Pharm. Bull.*, 32(3), pp.332–336.

Shimohama, S., Akaike, A. & Kimura, J., 1996. Nicotine-induced protection against glutamate citotoxicity. Nicotinic cholinergic receptor-mediated inhibition of nitric oxide formation. *Ann.N.Y.Acad.Sci.*, 777, pp.356–361.

Shin, E.J. et al., 2007. Repeated intracerebroventricular infusion of

nicotine prevents kainate-induced neurotoxicity by activating the alpha7 nicotinic acetylcholine receptor. *Epilepsy Res.*, 73(3), pp.292–298.

Søderman, A. et al., 2008. The nicotinic α7 acetylcholine receptor agonist ssr180711 is unable to activate limbic neurons in mice overexpressing human amyloid-β1-42. *Brain Res.*, 1227, pp.240–247.

Steiner, R.C., Heath, C.J. & Picciotto, M.R., 2007. Nicotine-induced phosphorylation of ERK in mouse primary cortical neurons: Evidence for involvement of glutamatergic signaling and CaMKII. *J. Neurochem.*, 103(2), pp.666–678.

Stevens, T.R. et al., 2003. Neuroprotection by nicotine in mouse primary cortical cultures involves activation of calcineurin and L-type calcium channel inactivation. *J. Neurosci.*, 23(31), pp.10093–10099.

Sukumaran, P. et al., 2012. Canonical transient receptor potential channel 2 (TRPC2) as a major regulator of calcium homeostasis in rat thyroid FRTL-5 cells: Importance of protein kinase C δ (PKCδ) and stromal interaction molecule 2 (STIM2). *J. Biol. Chem.*, 287(53), pp.44345–44360.

Sureshbabu, N. et al., 2010. Lipid-induced conformational transition of amyloid β peptide fragments. *J. Mol. Neurosci.*, 41(3), pp.368–382.

Suzuki, T. et al., 2006. Microglial alpha7 Nicotinic Acetylcholine Receptors Drive a Phospholipase C/IP3 Pathway and Modulate the Cell Activation Toward a Neuroprotective Role. *J. Neurosci. Res.*, 83, pp.1461–1470.

Toborek, M. et al., 2007. ERK 1/2 signaling pathway is involved in nicotine-mediated neuroprotection in spinal cord neurons. *J. cell. biochem.*, 100(2), pp.279–292.

Tong, M. et al., 2011. Role of key aromatic residues in the ligand-binding domain of alpha7 nicotinic receptors in the agonist action of beta-amyloid. *J. Biol. Chem.*, 286(39), pp.34373–34381.

Tu, S. et al., 2014. Oligomeric Abeta -induced synaptic dysfunction in Alzheimer ' s disease. *Mol. Neurodegener.*, 9(48), pp.1–12.

Utsugisawa, K. et al., 2002a. Over-expression of alpha7 nicotinic acetylcholine receptor induces sustained ERK phosphorylation and N-cadherin expression in PC12 cells. *Brain Res. Mol. Brain Res.*, 106(1-2), pp.88–93.

Utsugisawa, K. et al., 2002b. Overexpression of alpha7 nicotinic acetylcholine receptor prevents G1-arrest and DNA fragmentation in PC12 cells after hypoxia. *J. Neurochem.*, 81(3), pp.497–505.

Wang, H. et al., 2000. beta-Amyloid 1-42 Binds to α7 Nicotinic Acetylcholine Receptor with high affinity. *J. Biol. Chem.*, 275(8), pp.5626 –5632.

Wang, H.-Y. et al., 2000. Amyloid peptide Abeta(1-42) binds selectively and with picomolar affinity to alpha7 nicotinic acetylcholine receptors. *J. Neurochem.*, 75(3), pp.1155–1161.

Wang, H.-Y. et al., 2009. Dissociating beta-amyloid from alpha 7 nicotinic acetylcholine receptor by a novel therapeutic agent, S 24795, normalizes alpha 7 nicotinic acetylcholine and NMDA receptor function in Alzheimer's disease brain. *J. Neurosci.*, 29(35), pp.10961–10973.

Wang, J.Y. et al., 2003. Oxidative neurotoxicity in rat cerebral cortex neurons: Synergistic effects of H2O2 and NO on apoptosis involving activation of p38 mitogen-activated protein kinase and caspase-3. *J. Neurosci. Res.*, 72(4), pp.508–519.

Whalen, B.M., Selkoe, D.J. & Hartley, D.M., 2005. Small non-fibrillar assemblies of amyloid beta-protein bearing the Arctic mutation induce rapid neuritic degeneration. *Neurobiol. Dis.*, 20(2), pp.254–266.

Xue, S., Jia, L. & Jia, J., 2006. Hypoxia and reoxygenation increased BACE1 mRNA and protein levels in human neuroblastoma SH-SY5Y

cells. *Neurosci Lett*, 405(3), pp.231–235.

Yamamoto, N. et al., 2004. Environment- and mutation-dependent aggregation behavior of Alzheimer amyloid beta-protein. *J. Neurochem.*, 90(1), pp.62–69.

Yankner, B.A., Duffy, L.K. & Kirschner, D.A., 1990. Neurotrophic and neurotoxic effects of amyloid beta protein: reversal by tachykinin neuropeptides. *Science*, 250(4978), pp.279–282.

Yu, W. et al., 2011. α7 Nicotinic receptor activation reduces β-amyloid-induced apoptosis by inhibiting caspase-independent death through phosphatidylinositol 3-kinase signaling. *J. Neurochem.*, 119(4), pp.848–858.

Acknowledgement

From the very beginning, I would like to thank my thesis committee: Prof. Toru Asahi, Prof. Toshio Oshima, Prof. Kentaro Semba, and Dr. Naoya Sawamura, for their insightful comments and encouragement, but also for the hard questions which incented me to widen my research from various perspectives.

Undertaking this PhD has been a truly life-changing experience for me and it would not have been possible to do without the support and guidance that I received from many people.

I would like to express my sincere gratitude to my advisor Prof. Toru Asahi for the continuous support of not only my PhD study and related research, but also my career suggestion and life guidance, for his patience, motivation, and immense knowledge. I appreciate that Prof. Asahi always offered me as many opportunities as he can to expand my horizontals, to learn and experience the abundant colorful world since the undergraduate year 6 years ago. By grabbing every chance he provided, I was able to do the Alzheimer's disease related research in UCLA, experience the short time research program in Bonn University in Germany, and do the internship completely out of my research background in the start-up company at Silicon Valley. With the introduction and education by Prof. Asahi, I manage to acquire the research-related knowledge as well as business-related

knowledge such as some basic management, communication skills and the required knowledge of leadership and entrepreneurship, by taking the sub-major technological management leadership course and taking part in EDGE program. Meanwhile, I am grateful for the chances Prof. Asahi made to let me communicate with the professors, researchers, and students from other laboratories, universities or facilities, so that I can ponder my study from different angles after discussing with them. Prof. Asahi is not only the advisor in the research area but also the life guide for me. He advises on every concern I have about the career or life, and never judges or disagrees with me on the changeable thoughts along with 6 years. I could not have imagined having a better advisor for my PhD study.

My sincere thanks also goes to Dr. Naoya Sawamura, who has been my mentor for 6 years since I joined Asahi Lab. His support and continuous guidance, meticulous suggestions and astute criticism made my research project possible. Dr. Sawamura always plays a key role in encouraging and coordinating the whole project, from the undergraduate year through M.S. 2 years and PhD 3 years. I still remember the first time he gave me the papers and textbooks to teach me at first, and then let me start to self-learning the basic knowledge of molecular biology, biochemistry and neurochemistry etc, as well as the experimental techniques to do the research. He always keeps me abreast of the scientific developments. I am

grateful for him guiding at first and changing into discuss with me through years to arouse the independence of my scientific motivation. I appreciate him for offering me so many opportunities to participate in multiple conferences or symposiums, both in Japan and overbroad, to give oral speeches or poster presentations so that I could discuss with scientists or young researchers who are having the similar background of my research expertise. I am particularly thankful that Dr. Sawamura has been actively interested in my work and has always been available to advise me. I am very grateful for his patience, motivation, enthusiasm, and his scientific advice and knowledge, many insightful discussions and suggestions that, taken together, make him a great mentor.

I would also like to express thanks to Ms. Aiko Maeda and Ms. Hisae Nakanishi for their support of general affairs in daily life. My thanks also go to Prof. Hideko Koshima and Dr. Togo Shimozawa, senior Mr. Yoshiyuki Ogino and Mr. Kazuhiko Ishikawa for advising me at seminars and lab meetings, from both molecular biology and physical chemistry angles, which incent me to widen my research. I thank Dr. Takeyoshi Wada for being a gentle senior and a good friend for 5.5 years, teaching me experimental methods from the beginning, answering my questions whenever I have about research project, and advising me on different kinds of concern. I also thank previous senior Ms. Haruka Yamamoto-Yamada for teaching me at

the start step when I did not know how to start the experiment, taking care of me like a sister when we were in the same room together in the conference or symposium, and supporting me when I had career concern.

I am also thankful to my contemporary in the laboratory for 9 years' schoolfellow friendship, my group mate Satoru Wakabayashi and Akifumi Takanabe, Kenta Nakagawa and Udagawa Akihiro from physical chemistry group. I would like to thank my friends here in Japan as well, Nami Goto-Takada, Fei Xiong, Lei Yang, Huanqing Qi, Lu Yang, Zhengyuan Zhu, Yao Ju and all others who helped making my time in Japan pleasant and meaningful. I also thank my friends in China (Xiang Wei, Wei Zhang, Yun Hu, Jing Wang and all others) for supporting me spiritually, enlightening me when I am in my distress periods, and bringing me out from my loneliness.

Finally, I would express a deep sense of gratitude to my parents for supporting me spiritually throughout my PhD time and my life in general. I have an amazing family, unique in many ways. My parents' support has been unconditional all these years. I need to thank them in Chinese now...

独自来日至今 9 载，父母与我分隔两地，每逢佳节倍思亲而不得见，始终惦记。感谢父母在我独立成长的道路给予最大的支持，经济抑或是情感。纠结迷惘的时刻你们聆听与分享，孤单苦痛的时刻你们安抚与鼓励。无论漂泊多久多远，心中有家，就一直有那个最安全的避风港。谁言寸草心，报得三

春晖。感谢你们，予我生，教我长，力所能及地给我最好，还支持我冒险的梦想。路漫漫其修远兮，吾将上下求索。今后的漫长与艰辛，我将继续努力，因为你们，永远都是我奋斗的原动力。

早稲田大学　博士（理学）　学位申請　研究業績書

氏 名　　琚 曄　　印

（2017 年　2 月　現在）

種 類 別	題名、　発表・発行掲載誌名、　発表・発行年月、　連名者（申請者含む）
論文○	**Ju Y**., Asahi T., Sawamura N. (2014) Arctic mutant Aβ40 aggregates on α7 nicotinic acetylcholine receptors and inhibits their functions. *J Neurochem.* **131**(5):667-74.
講演	・ 国際学会（ポスター発表） **Ju Y**., Asahi T., Sawamura N. Arctic Amyloid beta inhibits CHRNA7's function by specifically binding to and aggregating on this membrane receptor. 10th International symposium on electrochemical micro & nanosystem technologies (EMNT2014)、沖縄、2014 年 11 月 **Ju Y**., Asahi T., Sawamura N. Arctic mutant Aβ modifies CHRNA7's functions through specific binding. Neuroscience 2013, 43rd Annual meeting of Society for Neuroscience, San Diego, USA,　2013 年 11 月 ・ 国内学会（ポスター発表） キョウ　ヨウ,朝日　透,澤村　直哉. Arctic Aβ による CHRNA7 の神経保護作用の抑制とその分子メカニズムの解析.　第 39 回日本分子生物学会年会、横浜、2016 年 12 月 ・ 国内学会（口頭発表） **Ju Y**., Asahi T., Sawamura N. Determination of the key domains of CHRNA7 in the interacting actions of Arctic mutant Aβ. 第 58 回日本神経化学大会、埼玉、2015 年 9 月 **Ju Y**., Asahi T., Sawamura N. Arctic mutant Aβ affects CHRNA7's functions. 第 56 回日本神経化学大会 (Neuro2013)、京都、2013 年 6 月 **Ju Y**., Asahi T., Sawamura N. Arctic mutant Aβ modifies CHRNA7's functions. 第 85 回日本生化学会大会、福岡、2012 年 12 月

早稲田大学　博士（理学）　学位申請　研究業績書

種 類 別	題名、　発表・発行掲載誌名、　発表・発行年月、　連名者（申請者含む）
講演	・ 国内学会（ポスター発表） **Ju Y**., Asahi T., Sawamura N. Arctic mutant Aβ modifies functions of CHRNA7.　12nd Conference for BioSignal and Medicine (CBSM)、山梨、2013 年 7 月 **Ju Y**., Asahi T., Sawamura N. Arctic mutant Aβ modifies CHRNA7's functions. 第 85 回日本生化学会大会、福岡、2012 年 12 月
その他（講演）	・ 国内学会（ポスター発表） キョウ　ヨウ,朝日　透,澤村　直哉. ニコチン性アセチルコリン受容体とアミロイドβタンパクの結合部位の検討.早稲田大学ナノテクノロジーフォーラム、東京、2016 年 3 月 **Ju Y**., Asahi T., Sawamura N. Aβ aggregation requires CHRNA7 as scaffold molecule. 日本薬学会第 132 回年会、札幌、2012 年 2 月 **Ju Y**., Asahi T., Sawamura N. CHRNA7 serves as scaffold molecule for Aβ aggregation. 2nd workshop for Diamond Researchers. 東京、2012 年 2 月 **Ju Y**., Asahi T., Sawamura N. CHRNA7 as scaffold molecule for Aβ aggregation. 第 54 回日本神経化学会大会、金沢、2011 年 9 月